Journal of Colloid and Interface Science 507 (2017) 453–469

Contents lists available at ScienceDirect

Journal of Colloid and Interface Science

journal homepage: www.elsevier.com/locate/jcis

Regular Article

Functional patterned coatings by thin polymer film dewetting

Andrew M. Telford [a,1], Stuart C. Thickett [b,1], Chiara Neto [c,*]

[a] Department of Physics, Imperial College London, London SW7 2AZ, UK
[b] School of Physical Sciences (Chemistry), University of Tasmania, Hobart, TAS 7005, Australia
[c] School of Chemistry and the Australian Institute for Nanoscale Science and Technology, The University of Sydney, NSW 2006, Australia

HIGHLIGHTS

- Emerging approach to fabricate micro-patterned polymer surfaces through thin film dewetting.
- Two applications of the approach in the biomedical and environmental fields.
- Advantages and potential future uses of the approach compared to other patterning approaches.

GRAPHICAL ABSTRACT

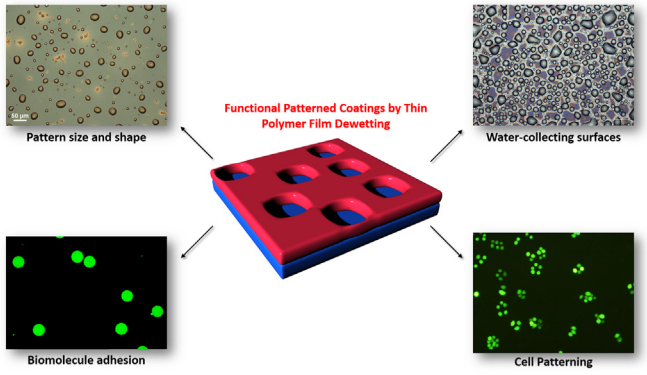

ARTICLE INFO

Article history:
Received 10 May 2017
Revised 28 June 2017
Accepted 2 July 2017
Available online 4 July 2017

Keywords:
Micro-patterning
Polymer coatings
Thin film dewetting
Self-assembly

ABSTRACT

An approach for the fabrication of functional polymer surface coatings is introduced, where micro-scale structure and surface functionality are obtained by means of self-assembly mechanisms. We illustrate two main applications of micro-patterned polymer surfaces obtained through dewetting of bilayers of thin polymer films. By tuning the physical and chemical properties of the polymer bilayers, micro-patterned surface coatings could be produced that have applications both for the selective attachment and patterning of proteins and cells, with potential applications as biomaterials, and for the collection of water from the atmosphere. In all cases, the aim is to achieve functional coatings using approaches that are simple to realize, use low cost materials and are potentially scalable.

1. Introduction

The formation of patterns on surfaces is a concept that finds application in numerous fields of science and technology: from microfluidics to biosensing, from the study of surface wettability to the design of energy-efficient materials. Several well-established methods exist to induce functional patterns on surfaces, including micro-contact printing, photolithography, and patterned plasma deposition. In an attempt to address some of the shortcomings of these techniques, namely high cost and little flexibility, an alternative class of patterning approaches has been developed in the last few decades, all relying on entirely spontaneous processes. For example, solutions of polymers (or polymerizable moieties) can be induced to form ordered surface patterns by controlling the evaporation rate and the solution viscosity. An intuitive example is the 'coffee ring' pattern, where material is deposited in concentric rings as a droplet evaporates. The approach has been developed to such an extent that arrays of hexagonally-packed dots or of parallel lines can be readily fabricated, by tuning

* Corresponding author.
E-mail address: Chiara.neto@sydney.edu.au (C. Neto).
[1] These authors contributed equally to this work.

http://dx.doi.org/10.1016/j.jcis.2017.07.004
0021-9797/

the type of solvent, type of polymer, polymer's molecular weight and temperature [1]. A second notable example of spontaneous patterning involves the use of so-called 'breath figures'. Put simply, breath figures are formed when a cold, hydrophobic surface is exposed to water vapor. Water condenses on the surface in small droplets, as it cannot form a film on it. The droplets grow in time, and spontaneously arrange in a variety of patterns. If breath figures are formed on thin films of polymer solutions, they will emboss their pattern into the liquid film. By controlling the relative rate of solvent evaporation to droplet growth and coalescence, monolayers of hexagonally-packed pores of similar sizes can be achieved [2]. A third example of spontaneous patterning technique, advanced by the Neto group, is the dewetting of thin liquid films [3–13]. This Feature article focuses on the work published in the Neto group concerning thin film dewetting of polymer bilayers, in particular for the fabrication of functional patterns in two applications: protein and cell patterning, and atmospheric water capture. The different fields of these two applications illustrate the wide scope of dewetting as a patterning method, and provides suggestions of other areas that might benefit from this approach.

Dewetting is the mechanism by which an unstable thin liquid film breaks up and retracts from a substrate on which it has been deposited. The forces that lead to dewetting in thin liquid films are intermolecular in nature, and therefore the majority of dewetting work focuses on thin films, with thickness on the order of 100 nm. An extensive literature exists on the fundamental understanding of wetting and spreading generally [14–22], and on the dewetting of thin polymer films more specifically [23–32].

The dewetting of thin polymer films is a remarkable tool to study the fundamental properties of the phenomenon, as the dynamics of dewetting can be tuned by tuning the viscosity of the polymers: temperature or exposure to appropriate solvents can be used to bring the polymers above their glass transition temperature, T_g, and allows studying them as they dewet in real time. Slowly flowing films allow the fabrication and optimization of patterns in a more straightforward way than, for example, films of simple liquids of low viscosity or stiff (e.g. metal) films. In addition, polymers offer a high variety of chemical functionality and mechanical properties, which account for their huge spread in materials science and in modern society.

Techniques such as spin coating, dip coating or spraying can be used to apply a non-wetting polymer film onto a substrate. The prepared film is therefore metastable or unstable, and, if taken above the T_g of the polymer, it will start to dewet until it reaches its equilibrium state, which is a series of isolated droplets with a finite Young contact angle (Fig. 1). The most commonly observed dewetting mechanism is heterogeneous nucleation, whereby holes appear at random locations in the film (Fig. 1(a)), their diameter grows with time (Fig. 1(b)), until the holes start to impinge on neighboring ones. Nucleation within the polymer film is due to the presence of chemical defects and/or dust [26], as well as residual stresses in the polymer due to the preparation method [33–35], and leads to a random distribution of holes. For very thin films (typically around 5 nm), a mechanism called spinodal dewetting can be observed that leads to a correlated pattern of holes, resulting from thermal fluctuations of the film's surface [36]. The polymer that has dewetted typically accumulates in a rim surrounding the hole, and the rim's shape and growth profile can be used to derive important viscoelastic and flow details of the system [30,37–39]. The rims of neighboring holes merge into cylinders of liquid, which finally break up by Plateau-Rayleigh instability into isolated droplets, usually placed along the lines of polygonal shapes created by the advancing rims (Fig. 1(c)).

In some circumstances, the Plateau-Rayleigh instability can be observed throughout the dewetting process and prior to the final stage, through the occurrence of viscous fingering inside the holes, and then the final pattern of droplets can be much denser and uniform across the substrate [40]. The occurrence of viscous fingering has been strongly related to a large liquid slip at the interface between the polymer melt and the substrate [11,41]. It has been argued that interfacial slip can be deduced by the morphological appearance of unstable hole rims and dewetted droplets formed by Rayleigh–Plateau instability [42], and the magnitude of slip depends on chain molecular weight. As expected, the specific chemical nature of the surface affects the magnitude of slip. In yet unpublished work, we have observed that the length of viscous fingers is strongly related to the molecular weight of the polymer [43]. This effect is qualitatively depicted in Fig. 2.

Dewetting dynamics, i.e. the study of the growth of nucleated holes as a function of time, is typically studied in the early stages of thin film dewetting (i.e. prior to hole coalescence) via time-lapse optical microscopy. The dynamics of dewetted hole growth has also been considered from a theoretical perspective by numerous research groups with distinct 'regimes' characterised by a different time dependence of the velocity of the dewetting front [44–51]. In the case of dewetting from a high-viscosity, solid substrate, the dewetting velocity is constant (i.e. hole growth is linear with time) and is a function of the surface tension and viscosity of the polymer, as well as the equilibrium contact angle the polymer makes with the underlying substrate. For the dewetting of very low viscosity polymers on solid substrates, viscous dissipation can be neglected and the dewetting velocity can be shown to have a $e^{-0.5}$ dependence, where e is the film thickness. Dewetting from low viscosity (liquid-like) substrates, a potentially important consideration in polymer bilayer systems, is usually characterized by a non-linear growth (typically radius $\propto t^{2/3}$) of nucleated holes due to viscous dissipation at the bilayer interface [46]. In the case of liquid–liquid systems, the dewetting velocity has a 2/3 power law dependence on the bottom layer thickness and a $-1/3$ power law dependence on the top (dewetting) layer [49]. Dewetting systems often exhibit both of these regimes (i.e. linear and non-linear growth) during the course of an individual experiment [50–52], due to changes in the dominant mode of energy dissipation at the interface.

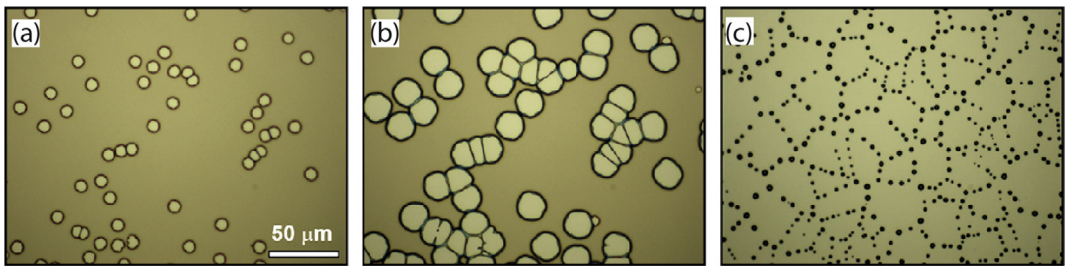

Fig. 1. Optical micrographs illustrating the main stages of dewetting of a thin polystyrene film (PS, 110 nm thick) on a hydrophobized silicon substrate by thermal annealing. (a) Holes nucleate at random locations in the film, (b) holes grow and start to coalesce with neighboring holes and producing cylinders of liquid, which (c) further decay into isolated droplets on the substrate.

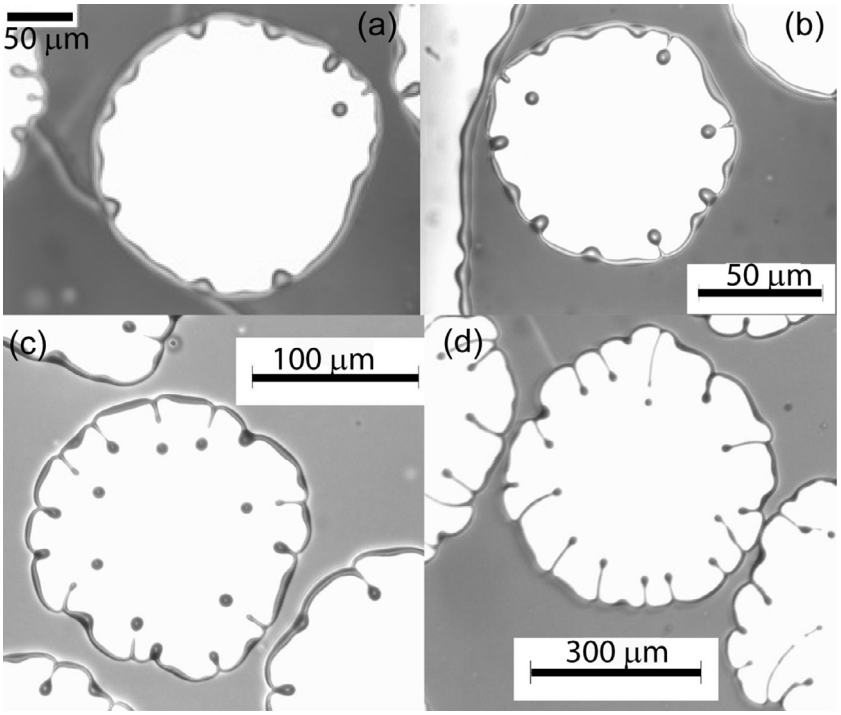

Fig. 2. Optical micrographs of the dewetting morphologies obtained in PS films retracting of hydrophobized silicon substrates, as a function of increasing PS molecular weight. The molecular weight is (a) PS 5.61 KDa, (b) 10.3 KDa, (c) 65 KDa, and (d) 125 KDa. Adapted from Ref. [43].

Interesting phenomena can occur in dewetting liquid systems. For example, a bilayer of liquid films can exhibit 'layer inversion', a rearrangement of the layer distribution due to the interplay of different viscosities and intermolecular forces in the system (we discuss this topic in Section 1.3). In some cases, dewetting can be observed in a single film of the same material. This phenomenon is referred to as 'autophobic dewetting', and occurs when a film of a certain material undergoes dewetting from a layer of identical molecules, somehow bound to the underlying substrate. For example, certain polymer films can dewet from polymer brushes of the same chemical composition attached to the underlying substrate [53,54]. Finally, certain amphiphilic molecules can transition from wetting a substrate to dewetting from it depending on the fine balance between their interactions with the substrate or with themselves. In these systems, a molecularly-thick layer could wet a substrate, but dewet if more layers of the same material are stacked onto the first, opening up applications molecular recognition on a surface [55].

1.1. Features of patterning by dewetting

Some of the positive features of thin polymer film dewetting for the fabrication of surface patterns are:

(i) *simplicity*; the pattern formation method is simple and does not require any specialized equipment, relying on the spontaneous retraction of the polymer film upon thermal or solvent annealing; in order to obtain reproducible results in a research laboratory, the substrate and the polymer solution need to be clean from contamination, both chemical and particulate;

(ii) *versatility*; the patterns that are formed by dewetting of polymer bilayers lead to both chemical and topographical patterns; there is no restriction on the choice of synthetic polymers used to fabricate the bilayers, so tailored contrast can be achieved between the background and the pattern (wettability, mechanical, conductive, functional); with our recent work, we have shown that even stable films can be made to dewet upon exposure to mixtures of vapors of good and poor solvents; [11,12] the size of the produced patterns (holes or droplets) can be easily varied between a few hundred nanometers and a few hundred micrometers, by varying film thickness or dewetting time;

(iii) *scalability;* thin polymer films can be applied to both large and 3D substrates, and this means that many substrates can be patterned by dewetting, including for example prosthetics, catheters, large plastic sheets and other devices; in a research laboratory coating may be fabricated via spin-coating, whereas dip-coating and spraying would facilitate the creation of larger patterned substrates;

(iv) *easy control over pattern dimension and distribution*; in clean conditions, the dewetted holes nucleate all at the same time, so are produced in a narrow size range (typical size variation between 1 and 10%), and the final dewetted pattern of droplets has reproducible size (variation up to 10%) and distribution density; the density of nucleated holes increases with increasing polymer molecular weight, attributed to a greater level of internal stress within higher molecular weight films during the coating process; [35]

(v) *low cost*; the polymers that can be used to produce functional patterns are many, low cost and easily (often commercially) available. Furthermore, the equipment required is relatively basic, which makes the patterning accessible to a wide range of users, including non-experts in polymers and wetting. Our very rough cost estimate for patterning small substrates in a research laboratory is around USD 0.10 per sample for dewetting, compared to USD 0.50 per sample for photolithography, mainly due to the higher cost of equipment in the latter case.

The rich variety of possible applications and the ease of use of dewetting will be discussed throughout this paper, and additional

advantages specific to the use will be highlighted. On the other hand, patterning by dewetting has three main disadvantages compared to other patterning techniques: (1) the smallest feature size (droplet or hole) that can be produced is in the range of hundreds of nanometers, well below the capabilities of photolithography or micro-contact printing; (2) in the absence of pre-patterning, dewetting is rather limited in the number of possible shapes or order that can be produced; (3) it is necessary to work with thin films (of the order a few tens to a few hundred nm) in order to obtain a pattern in a timely manner, which limits stability to scratches from sharp objects.

Some of the limitations that are intrinsic to dewetting have been addressed in the literature, and the result is that thin film dewetting is even more widely applicable as a patterning platform. In the following Sections, the introduction of solvent annealing and pre-patterning of the substrates is discussed as important steps towards widening the scope of application of polymer dewetting.

1.2. Experimental considerations in the design of micro-patterned surfaces via dewetting

There are some disadvantages or technical challenges in the use of dewetted bilayers, which should be taken into consideration in surface design (see Fig. 3). In order to prepare the initial bilayer via a technique such as spin coating, the top layer must be soluble in a non-solvent for the bottom underlayer. This is to avoid polymer mixing and dissolution of the bottom layer during deposition of the top layer, and while this sounds straightforward, judicious choice of solvents is important. In our work using polystyrene (PS) as an underlayer, we typically spin-coat our top layer from ethanol or acetonitrile to avoid underlayer dissolution. We also generally restrict our studies to polymers that are glassy at room temperature (i.e. they have a high glass transition temperature, T_g); this enables one to take advantage of the mechanism of dewetting only occurring above room temperature, where polymer chains have sufficient mobility. From a synthetic perspective this restricts our choice of polymers typically to styrenics, certain methacrylates, poly(*N*-vinylpyrrolidone) and members of the poly(vinylpyridine) family; [56] recently we have also explored the possibility of preparing hydrophobic base layer polymers with high T_g via the copolymerization of a fluorinated monomer (2,3,4,5,6-pentafluorostyrene) with *N*-phenylmaleimide to incorporate chain-stiffening groups such as heterocycles into the polymer backbone [57].

An additional consideration in the design of polymer bilayer films to generate micro-patterned substrates is the relative molecular weights of each layer, as this can result in different final surface morphologies than the desired surface of isolated polymer droplets. If thermal annealing of the bilayer is performed above the T_g of both polymers, the melt state viscosity η_0 (and its power law dependence on polymer molecular weight [58–60], $\eta_0 \propto M^{3.5}$) becomes of critical importance, as a liquid–liquid dewetting regime can potentially arise. In such a case the polymer underlayer is equivalent to a deformable substrate; this is further complicated by layer inversion, discussed in Section 1.3.

1.3. Layer inversion in polymer bilayers

The Neto group has pioneered the use of patterns generate by the dewetting of polymer bilayers. The choice of polymer bilayers as a platform for pattern formation was brought about by the great versatility and ease of preparation: polymers are available in almost infinite chemical variety, and most of them can be spun or dip-coated into smooth coatings on solid substrates. The dewetting of polymer bilayers enables the formation of polymer patterns of varied chemistry and material properties.

However, the dewetting of polymer bilayers by thermal annealing at a temperature above both polymers' T_g, often brings about an undesired side-effect, called layer inversion, as depicted in Fig. 4. When the bottom polymer layer has a lower surface tension than the top layer, it will migrate to the film/air interface and partially coat the top polymer layer during the dewetting process. Layer inversion can be easily confirmed based on the morphological features of the dewetted patterns, mostly that the dewetted droplets are no longer isolated from each other, but still connected by a cylinder, as shown in Fig. 4(d). In more quantitative experiments, the top layer can be dissolved in a selective solvent, and the

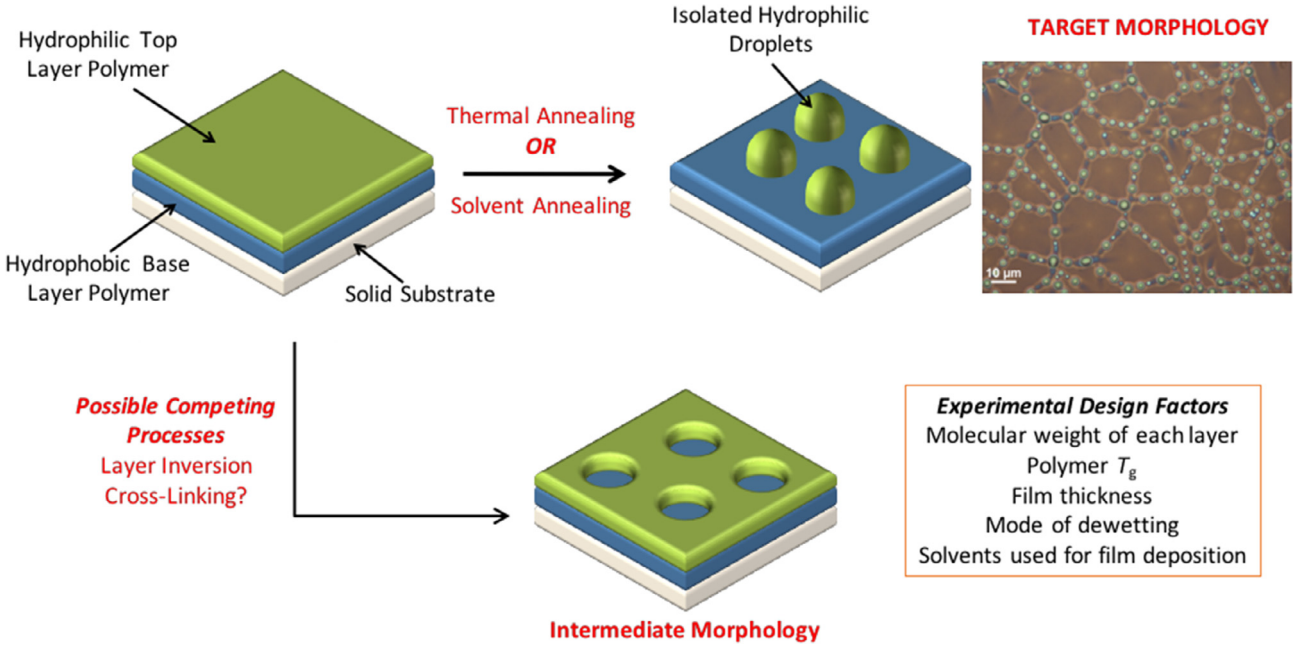

Fig. 3. Schematic overview of polymer bilayer dewetting for the creation of patterned surfaces.

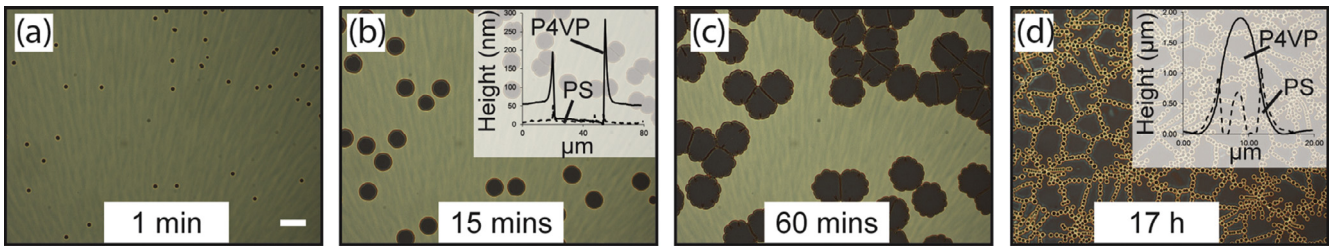

Fig. 4. Optical micrograph of the dewetting of a poly(4-vinylpyridine) (P4VP) film (43 nm) on top of a PS film (96 nm) upon thermal annealing at 180 °C; the time stamps indicate increasing time of annealing (scale bar = 50 μm). Insets: AFM cross-sections of the same samples before and after selective dissolution of the top P4VP with ethanol, the dashed line indicating the topography of the bottom PS film imaged after dissolution of the top P4VP.

exposed topography can be imaged by atomic force microscopy (AFM), as shown in the insets in Fig. 4(b) and (d).

The competition between film dewetting and layer inversion was explored by the Neto group through the dewetting of poly (4-vinylpyridine) (P4VP) from PS where the molecular weight of each layer was varied [4]. When a 'liquid-on-solid' dewetting regime was employed (low molecular weight P4VP on top of high molecular weight PS), complete dewetting of the P4VP film into isolated droplets was achieved upon thermal annealing. In contrast, liquid–liquid dewetting systems (i.e. the bottom layer has a lower melt viscosity than the top layer) demonstrated a cessation in hole growth prior to coalescence, in addition to other observed phenomena (jagged and irregular hole profiles, as well as local variability in the thickness of the unperturbed P4VP film). A non-constant hole growth profile was also observed in liquid–liquid cases, as predicted from modelling of liquid–liquid dewetting [49]. The arrested hole growth prior to full dewetting was attributed to layer inversion due to the higher mobility of the PS underlayer in the melt state and exposed domains due to hole nucleation in the top P4VP layer. This was confirmed via selectively dissolving the top P4VP layer in ethanol followed by tapping mode AFM. A competitive model describing these two processes was put forward, comparing the predicted reptation time for the PS used to the shear rate of the dewetting front [61], which was in good agreement with observations. In order to reach fully dewetted patterns of P4VP droplets on top of the PS film, the rate of dewetting needed to be significantly greater than the rate of polymer migration via reptation.

1.4. Effect of solvent vapor annealing on polymer film dewetting

The majority of the work published on polymer film dewetting involves films of thickness around or below 100 nm, as the driving forces that are exploited for dewetting are mostly intermolecular in range, and can act only over relatively thin films (van der Waals forces, electrostatic forces, hydrogen bonding) [36,45,62–64]. Very thick films do not dewet via thermal annealing. However, in recent work, the Neto group has demonstrated that films thicker than 600 nm can be readily dewetted, if the annealing mechanism is changed from thermal annealing to solvent annealing [11,12]. The main motivation behind this work was to produce polymer droplets onto substrates with size ranging from a few hundred nanometers to a few hundred micrometers, with narrow size distribution in each case, and without altering the substrate properties. This aim was successfully achieved by employing the effect of replacing thermal annealing with solvent annealing, using a mixture of vapors of good and poor solvents to anneal the polymer films.

In our first paper studying solvent annealing, the dynamics and morphology of dewetting of PS films on silicon substrates were investigated upon the exposure to vapor mixtures of toluene, a good solvent for PS, and ethanol, a non-solvent for PS [11]. Adding a small amount of ethanol vapor to the saturated toluene vapor resulted in a dramatic increase in dewetting rate of the PS films, an increase in the contact angle of PS droplets and hole rims on the substrate, and extensive fingering leading to droplet shedding. The increase in dewetting rate upon addition of a non-solvent for the polymer was initially puzzling, but was soon revealed to be due to the collapse of polymer chains, an effect that had been predicted in theoretical studies [65,66], but measured in few experiments [67–69]. Our experiments confirmed the theoretical prediction that in the presence of a mixture of a good solvent and a non-solvent the PS chains collapse into a globule conformation, which leads to a greatly reduced viscosity. At the same time the experiments revealed clear signs of a large interfacial slip, which, combined with the large increase in contact angle of the PS on the substrate, pointed to the presence of a thin film of ethanol adsorbed on the silicon oxide substrate. The value of slip length obtained in the presence of ethanol vapor was of the same order as the values obtained for PS on hydrophobized silicon [48]. The mechanisms of chain collapse and interfacial slip within the same experiment could not be decoupled, and this remains a question that needs addressing. The direct and practical consequence of the large increase in the driving forces for dewetting was that much thicker films (up to 800 nm thick) could be dewetted than in dewetting experiments relying only on van der Waals forces, and therefore very large polymer droplets could be created, as shown in Fig. 5 and discussed in Section 3.2.

In our second paper the solvent annealing approach was expanded to bilayers of thin polymer films. A top film of P4VP film was cast on a bottom PS film on silicon substrates, and the bilayer was exposed to vapors of binary and ternary mixtures of ethanol,

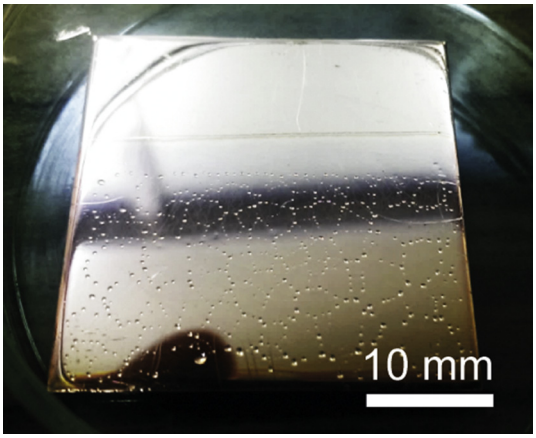

Fig. 5. A dewetted pattern obtained by solvent annealing of an 800 nm thick PS film on top of a plain silicon substrate. The average PS droplet size visible by eye is around 80 μm. Reprinted with permission from Ref. [12]. Copyright 2016 American Chemical Society.

acetone and water, respectively a good solvent, a poor solvent and a non-solvent for P4VP. This paper confirmed the dramatic increase in dewetting rate upon adding poor solvents, established that the driving force for dewetting is stronger the poorer the quality of the solvent for the polymer film, and identified the individual roles of the three solvent vapors in the mixture. Ethanol, as a good solvent for P4VP, acts as the plasticizer, which enables the P4VP to flow by lowering the film viscosity (acetone, as a poor solvent, has a similar effect but to a lesser extent). Water, as a non-solvent for P4VP, drives the dewetting faster, by inducing the collapse of the P4VP chains and dramatically reducing the polymer viscosity (acetone, as a better solvent than water, has a similar effect but to a lesser extent). Finally, acetone, as a poor solvent for P4VP but a good solvent for PS, preferentially adsorbs to the PS substrate, inducing a lubricated flow of the P4VP on the PS. An added benefit observed was that the layer-inversion of the P4VP film with the bottom PS film, an effect associated with annealing bilayers due to the lower surface tension of PS [4], was prevented by tailoring solvent vapor annealing conditions.

The practical consequence of these studies was that topographical and chemical patterns, consisting of hydrophilic P4VP bumps on hydrophobic PS background, were fabricated, with a bump diameter and height tunable within almost two orders of magnitude (1–80 μm and 40–9000 nm, respectively), and with a distribution density tunable by 5 orders of magnitude. These patterns were used effectively as platforms for the capture of atmospheric water, as described in Section 3 below.

1.5. Inducing ordered dewetting through micro-contact printing and templating

One of the perceived limitations of polymer film dewetting as a patterning approach is the inability to create a pattern with spatial order and controlled droplet size. However, numerous studies have shown that dewetting can be well controlled using numerous stimuli, which lead to ordered and highly reproducible surface patterns. A recent review has covered several of these approaches [70]. Here two approaches that were explored by the Neto group will be discussed, the first involving the use of stamps in micro-contact printing, and the second involving sacrificial colloidal templates. In the first of these publications [71], a polydimethylsiloxane (PDMS) stamp was used to hydrophobize silicon wafers (coating them with a monolayer of octadecyltrichlorosilane, OTS) along a square array pattern, followed by subsequent spin-coating of PS on top of the pattern. Interestingly, although PS films cannot be directly spin-coated over OTS-coated silicon wafers, as the contact angle of the PS solution is too high, the films can be directly spin-coated on the patterned OTS layer, as the contact angle hysteresis of the solution contact lines allows for a uniform film to be deposited. This work demonstrated that ordered dewetting patterns can be obtained by pre-stamping the substrate with ordered chemical monolayers; the type of patterns that can be formed are either channels in the PS film (at early stages of dewetting), or ordered arrays of PS droplets (in final stages of dewetting) (see Fig. 6). A partial bleeding out of the silane layer was seen as responsible for the complete dewetting of the films, including on parts that were not coated in OTS.

In the second publication, colloidal crystals, made up of a single sized silica colloid suspension or a mixture of two sizes, were used as sacrificial templates to guide the controlled nucleation of holes within the top P4VP film of a polymer bilayer [10]. In this study, the location on the film at which holes nucleate and grow was determined by the position of micro-scale colloidal particles, compacted into close-packed arrays. The colloidal particles could sink into the top P4VP film by pre-annealing, and then washed away, creating an indented, ordered array of holes on the P4VP surface. Although the pattern of nucleated holes at the indentation stage was highly ordered and matched well the pattern of the colloidal crystal, the order of the pattern was gradually lost as the holes grew, and the final positions of holes at the point of coalescence with neighboring holes was regular but no longer ordered (Fig. 7). As the bilayer was thermally annealed to induce the growth of the nucleated holes, layer inversion in the bilayer had to be delayed or prevented.

2. Applications of dewetting in protein and cell patterning

Many types of tissue cells require both chemical and mechanical cues from their surroundings to proliferate and differentiate, and they may undergo *apoptosis* (programmed death) in their absence. When culturing cells *in vitro*, it is necessary to provide optimal adhesion conditions on the culturing plate. The interaction of a cell with its surroundings *in vivo* is often mediated by a scaffold of proteins (the extra cellular matrix, ECM) that can provide specific chemical cues (in the form of specific sequences of amino acid residues) and mechanical stiffness [72]. The three-dimensional ECM can be simulated in two dimensions by coating a flat surface with a patterned layer of ECM proteins specific to the type of cells that are cultured [73].

ECM proteins can be patterned onto a surface to provide isolated domains that are adhesive to cells, usually embedded in a film that is cell-repellent. Patterns with features of size comparable to the cell size have important applications in biomedicine and tissue engineering [74]. For example, cell studies on models such as tumor spheroids require control over the size of the cell colony, i.e. the number of cells attached to a specific site on a surface

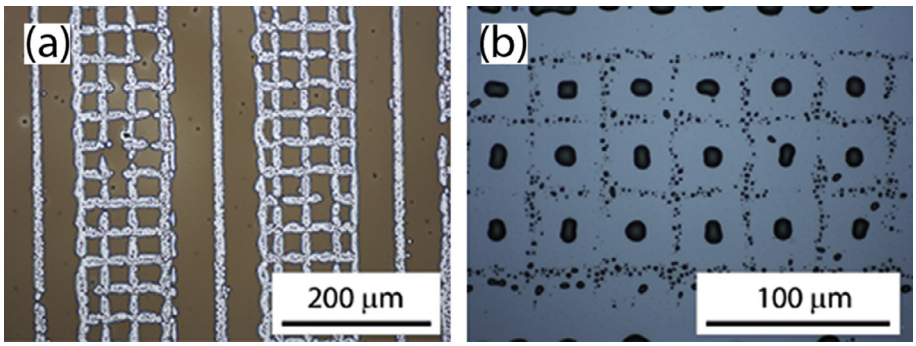

Fig. 6. Ordered patterns obtained by dewetting of polystyrene films on pre-patterned silicon substrates above the T_g of the polymer. (a) Intermediate dewetting pattern resulting from low-temperature (70 °C) annealing. (b) Final dewetting pattern resulting from high-temperature (100 °C) annealing. Reprinted with permission from Ref. [71]. Copyright 2012 American Chemical Society.

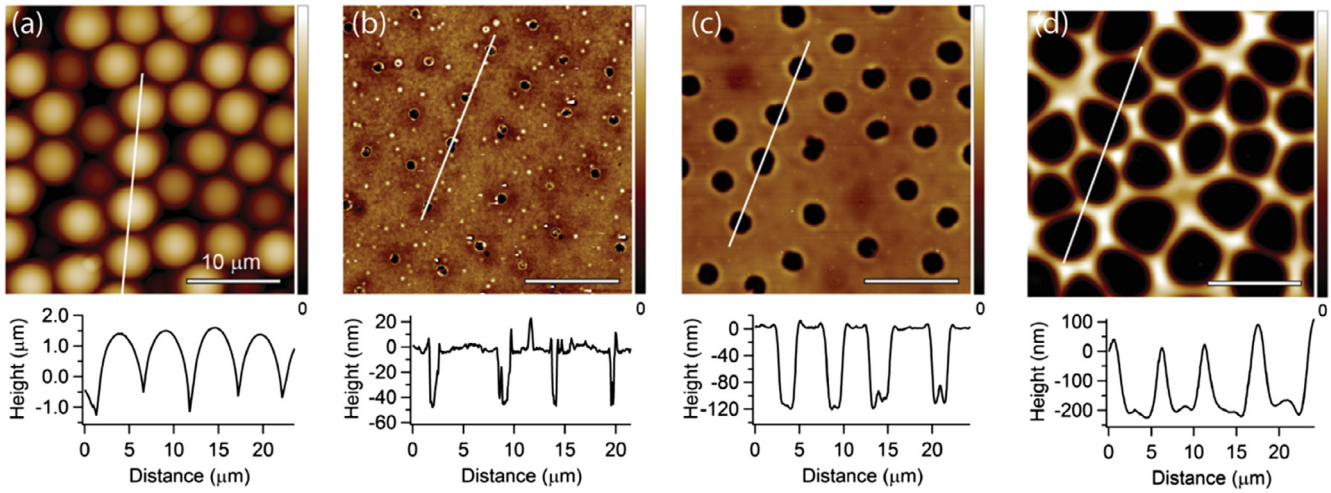

Fig. 7. AFM micrographs of (a) a single-particle colloidal crystal assembled on a P4VP/PS bilayer. (b)–(d) AFM micrographs of the same area of a micropatterned P4VP/PS bilayer after (b) colloidal imprinting at 80 °C for 1 min, and (c)–(d) annealing at 190–210 °C for increasing times. The same area was imaged *in situ* in parts (b–d). Cross sections of the AFM topography images are shown below each image. Reprinted with permission from Ref. [10]. Copyright 2015 Wiley.

[75]. In different instances, attachment and confinement of a single cell on a surface is required [74]. Both these scenarios are possible on patterns of adhesive domains with lateral dimensions in the tens of micrometers. In the growth of tissues *in vitro*, it is sometimes required to control the density of individual cells onto a surface, which can be achieved by tuning the density of adhesive sites [76]. More complex tissues often require the growth of co-cultures of multiple cell types, where the degree of homotypic (same cell) and heterotypic (different cells) contact is key [77,78].

Patterning of surfaces by dewetting of polymer bilayers is particularly suitable to the examples described above. The round holes produced upon dewetting of a thin film expose the underlying surface. The top (dewetted) film and the bottom film (exposed inside the holes) can be chosen to interact very differently with proteins and cells. For example, if the bottom film is protein adhesive and the top film is protein repellent, the resulting pattern will promote adhesion of ECM proteins, and subsequently cells, exclusively inside the holes [3]. The ability to easily control the diameter of the holes and their density on a surface allows the confinement of cell clusters of controlled size (from single cell upwards) with tunable inter-cluster distance. Using customizable polymer chemistry, the patterns of holes can be further modified to promote adhesion of a second type of cell after adhesion of the initial clusters, to produce co-cultures with tailored contact.

2.1. Polymer bilayers and protein patterning

Protein adhesion onto a surface is of paramount importance in the interaction of biological and non-biological matter. Cells attach to surfaces and to each other via layers of proteins and other macromolecules. Strongly adsorbed proteins can change their native conformation by exposing their hydrophobic domains to hydrophobic surfaces, or their charged domains to charged surfaces, or dehydrate [79]. Certain conformations of adsorbed proteins on a surface can promote cell attachment, and elicit healthy growth or an uncontrolled inflammatory response. Therefore, coatings for biomedical applications require control over the conformation of adsorbed proteins. When patterning of cells onto a surface is required, localized seeding of proteins is an excellent strategy. Polystyrene (PS) is one of the most commonly used substrates for the adhesion of several physiologically-relevant proteins. In the work of the Neto group thin PS films were used as a base layer onto which a dewettable layer was cast. Proteins bind to PS via hydrophobic interactions, and some of our studies suggest that most adsorbed proteins retain their ability to promote healthy cell growth (see Sections 2.2 and 2.3). Moderate contrast in protein adhesion was achieved when poly(methyl methacrylate) (PMMA) or poly(*N*-vinyl pyrrolidone) (PNVP) were dewetted from PS [3,7]. Both PMMA and PNVP are moderately hydrophilic polymers (relative to PS), and their ability to trap a thin layer of water on their surface is the likely cause of their moderate non-fouling properties (relative to PS) [80]. PNVP performs better than PMMA as it is more hydrophilic (contact angle with water is 16° on PNVP, and 75° on PMMA). Fabricating a PNVP coating, however, requires an additional step as the PNVP is water-soluble. We discovered that heat treatment caused cross-linking of PNVP: [81] complete cross-linking of thin films at 200 °C for 30 min; partial cross-linking at lower temperatures. Hence a careful choice of annealing temperature of PNVP/PS bi-layers produced dewetted patterns with cross-linked, water-insoluble PNVP, suitable for protein adhesion studies.

The data in Fig. 8 exemplifies the contrast in protein adhesion obtainable using a simple pattern of dewetted PNVP on top of flat PS. Collagen I was incubated onto the patterns, and attached preferentially onto the PS domains, inside the dewetted holes. This is obvious from the fluorescence micrograph in Fig. 8(b), where the proteins were tagged with fluorescein isothiocyanate (FITC). The contrast in protein adhesion is also visible by comparing AFM images of the PS surface (Fig. 8(c)) and the PNVP surface (Fig. 8 (d)) after incubation with the collagen I solution (10 μg/mL). This low concentration is sufficient to drive endothelial cell attachment (see Section 2.3), hence the PNVP/PS system has potential applications in tissue engineering. Higher concentrations of collagen I would lead to attachment onto PNVP as well, however we found that PNVP was exceptionally repellent to fibrinogen and immunoglobulin G, up to 1 mg/mL in concentration [81]. Our results highlight the complexity of the protein-surface interaction, and how different proteins can behave very differently when contacting a surface. Protein fouling is hence not universal, but rather specific to the type of protein, and should be tested for specific applications [82].

2.2. Patterning of grafted polymer layers

The contrast of protein adhesion in dewetted patterns can be dramatically improved by selective post-modification of the

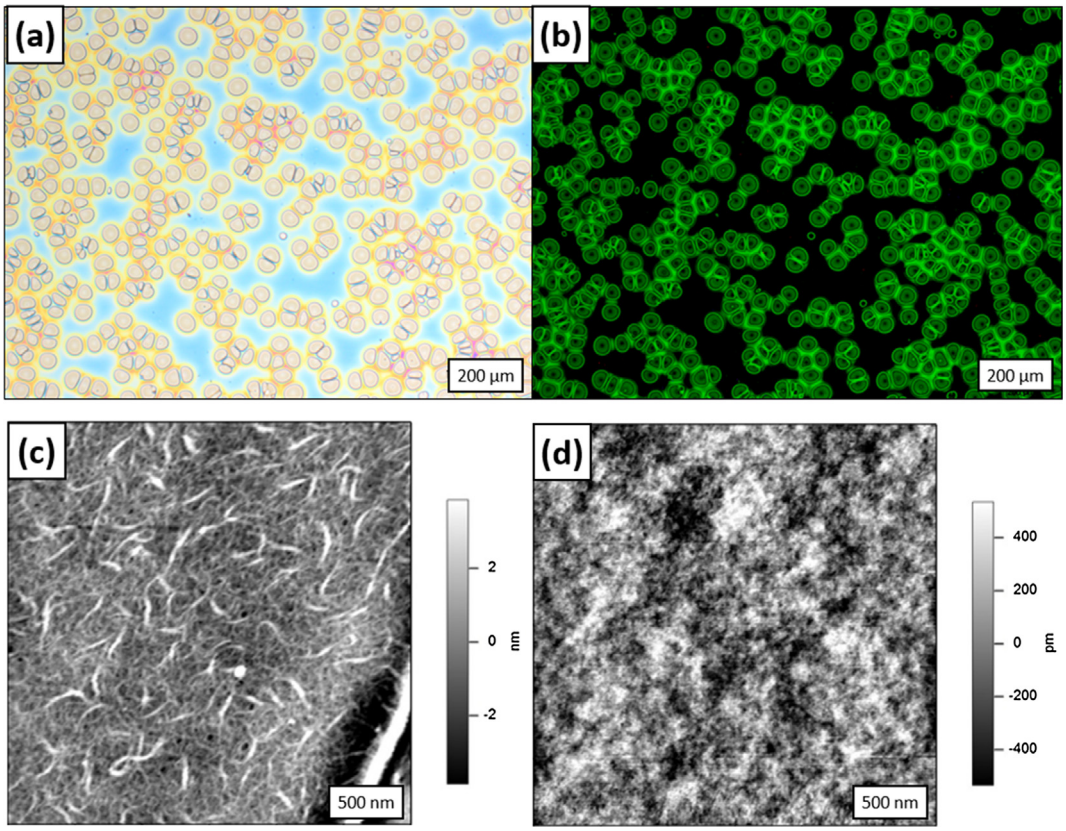

Fig. 8. Adsorption of collagen I onto PNVP/PS dewetted patterns. (a) Bright field and (b) fluorescence optical micrographs of FITC-tagged collagen I onto a dewetted pattern. The green fluorescent protein is only visible inside the dewetted holes. AFM micrographs of (c) PS domains inside the dewetted holes and (d) PNVP layer outside the holes. Collagen I is visible on the PS surface as elongated, worm-like aggregates, while it cannot be detected on the surface of PNVP. Adapted from Ref. [7] with permission of The Royal Society of Chemistry. (For interpretation of the references to colour in this figure legend, the reader is referred to the web version of this article.)

coating. The approach in the Neto group has involved grafting protein-repellent polymer layers, i.e. by tethering polymer chains with a functional terminus onto a surface by various methods. When the chains are densely-packed, they are forced to extend away from the substrate, in a "polymer brush" conformation, dictated by the balance between the steric hindrance from neighboring chains and the elastic recoil of the chains. The mechanical properties of polymer brushes depend strongly on their solvation state [83]. In biomedical applications, polymer brushes are usually hydrophilic, and swell in water-based biological media. Such swollen brushes become elastic layers dense enough to prevent protein permeation and elastic enough for large bodies such as cells to bounce off [84]. Most importantly, by trapping water they prevent the very first step of irreversible protein (and subsequent cell) adhesion, which includes the partial dehydration and denaturation of the protein and its intimate interaction with the substrate (by Van der Waals and electrostatic forces) [80].

Grafting of polymer chains can be obtained by physisorption (where the tethering group adsorbs to the substrate) or by chemisorption (where the tethering group bonds chemically with the substrate). Chemisorbed brushes are more stable than physisorbed ones to immersion, shear and temperature variation, and can be produced by "grafting-to" or "grafting-from" approaches. In the following, we will describe examples of each to produce patterned brushes in combination with dewetting.

The grafting-from approach is often referred to as "surface-initiated polymerization", and it requires the immobilization of polymerization initiators onto the substrate, from which polymer chains can be grown by monomer addition [85]. Densely-packed grafted layers can be achieved by controlling the density of the initiator on the surface. To grow a polymer brush with controlled thickness and mechanical properties, the dispersity of the polymer chain lengths must be minimized. Various approaches to the reversible deactivation radical polymerization of vinyl monomers are available, one of which is atom transfer radical polymerization (ATRP) [86]. In this technique, a radical initiator (typically a halogenated ester) initiates the growth of a polymer chain in the presence of a transition metal (typically copper) catalyst. The careful control of the rate of association and dissociation of the carbon-halogen bond at the growing end of the chain, allows exquisite control over the chain length distribution. The reactive halogen group at the end of each growing chain allows post-modification of the surface of the polymer brush. In our approach, surface-initiated ATRP was combined with patterning by dewetting, to produce surfaces with protein-adhesive domains in a highly protein-repellent background [6]. We employed a particular variation of ATRP, named activators generated by electron transfer (AGET-ATRP) [86]. The standout advantage of this variation is the use of a mild reducing agent, such as ascorbic acid, to establish the optimal ratio between the oxidized and reduced forms of the copper catalyst, which is paramount to the control over the polymerization. The added advantage is that the reaction can potentially be carried out in the presence of oxygen, which usually inhibits radical-based process, but is instead scavenged by the reducing agent. Overall, AGET ATRP is a robust approach to grafting of polymer brushes.

As seen in the scheme in Fig. 9, the system was based on a bilayer of polymer thin films. Protein-adhesive PS was used as the bottom layer. A film of a custom-made polymer, containing in its structure the ATRP initiator 2-bromopropanoate, was

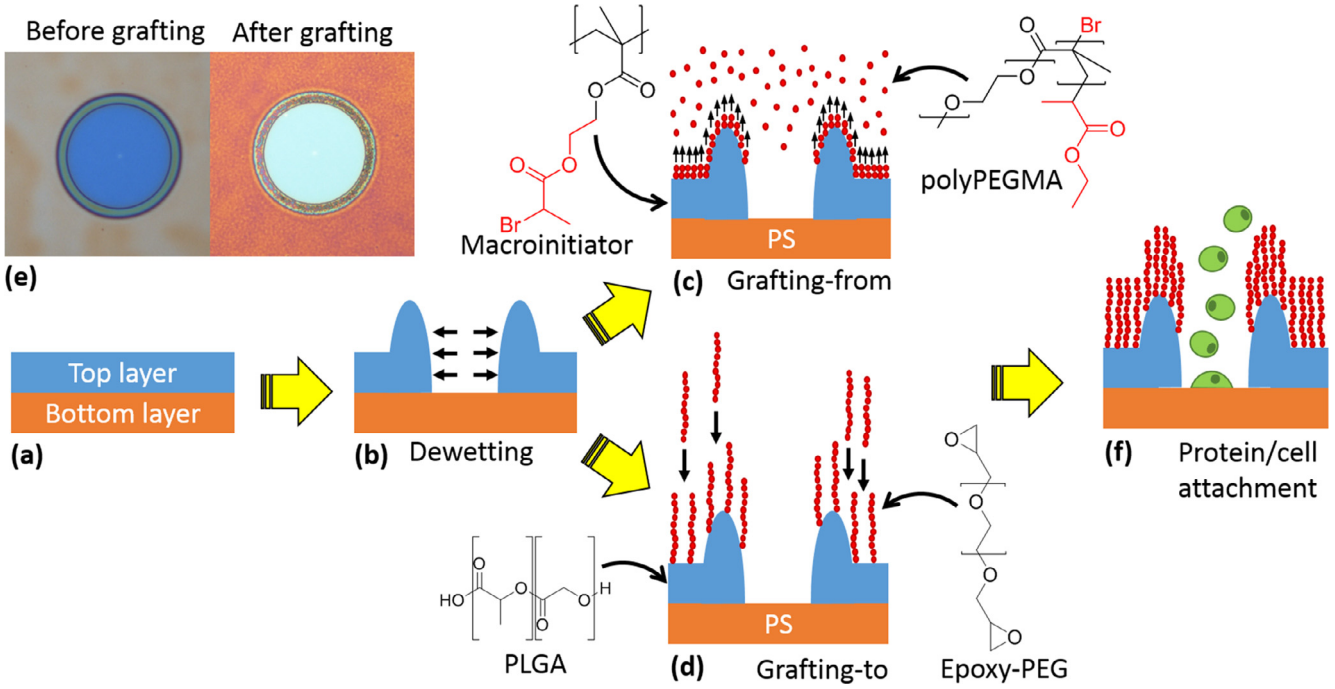

Fig. 9. Patterning of polymer brush by dewetting. The polymer thin film bilayer (a) is patterned by dewetting (b); non-fouling polymer chains are either grown from the top layer (grafting-from, c) or pre-synthesized and then tethered to the top layer (grafting-to, d); the grafting does not affect the pattern (e); the patterned polymer brush allows protein and cell attachment only on the domains where the bottom layer is exposed (f).

subsequently deposited on top of the PS. This polymer, from here on referred to as the "macroinitiator", was based on a poly(methyl methacrylate) backbone, which easily dewets from PS. After dewetting was used to achieve the desired pattern in the macroinitiator bilayer, a hydrophilic brush of poly[poly(ethylene glycol) methyl ether methacrylate] (polyPEGMA) was grafted from the macroinitiator film using AGET-ATRP [8]. The initiator was distributed homogenously across the thickness of the film, and some monomer could access deeply-buried initiators and begin the growth of buried chains. The result was a strongly intermixed layer of macroinitiator and brush, topped by the pure brush. The simultaneous brush growth and interpenetration of macroinitiator and brush chains produced a non-linear increase of the brush. Nevertheless, the brush thickness in our system was precisely controllable [6].

Poly(PEGMA) brushes grafted from our custom-made macroinitiator could be grown up to ~70 nm thick, and exhibited excellent protein and cell repellent properties [6]. Above this thickness delamination from the substrate started to occur. Shown in Fig. 9 (e) are optical micrographs of a dewetted macroinitiator film onto PS, before and after grafting of poly(PEGMA), showing no alteration of the pattern. The outstanding contrast in protein adhesion achievable with patterned brushes can be observed in Fig. 10. Bovine serum albumin (BSA), tagged with the green florescent

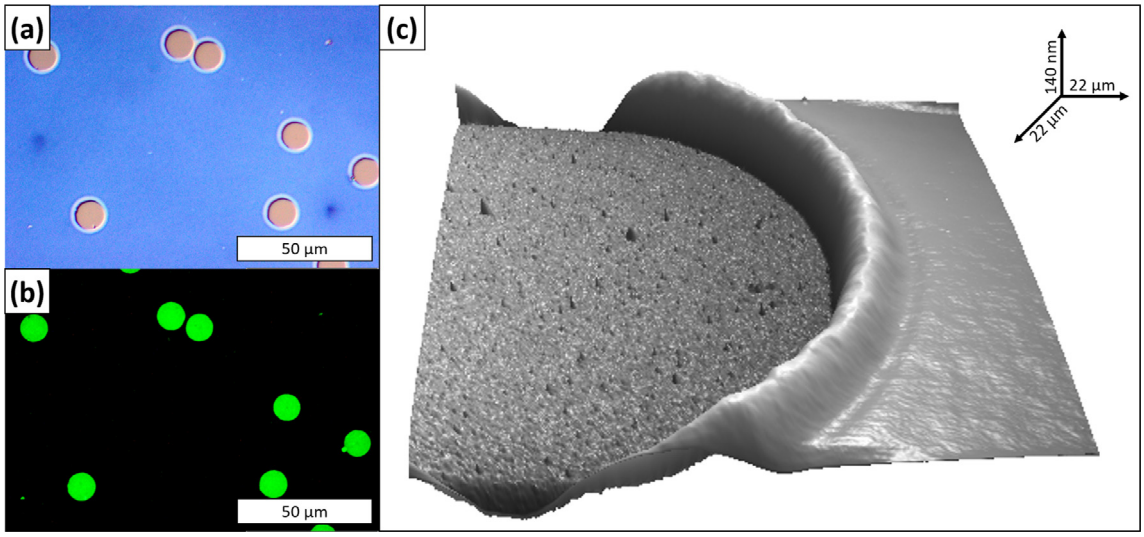

Fig. 10. Protein adhesion onto a dewetted poly(PEGMA) brush, grafted from a macroinitiator layer. (A) Bright field and (B) fluorescence optical micrographs of FITC-tagged BSA adsorbed onto the patterned brush. BSA adsorbs only in the adhesive holes, where the base polystyrene layer was exposed, and not on the poly(PEGMA) brush. (C) 3D AFM image of a single dewetted hole after exposure to BSA: the protein could be detected only inside the dewetted hole by the high surface roughness of the area, while not on the outer polyPEGMA brush, which remained smooth.

dye FITC, was deposited onto a patterned poly(PEGMA) brush. Despite the high concentration of the protein solution (1 mg/mL), no protein adhesion was detected on the polymer brush (areas outside the dewetted holes), while a strong fluorescent signal from adsorbed proteins could be seen inside the dewetted holes (Fig. 10(a) and (b)). AFM confirmed the presence of a layer of adsorbed protein inside the holes, detectable from its high roughness, but not on the surrounding polymer brush, which appeared smooth (Fig. 10(c)). This is an outstanding improvement over simpler systems (such as dewetted PMMA or PNVP, see Section 2.1), where moderate adhesion contrast was possible only for protein concentrations in the tens of μg/mL.

In the grafting-to approach for the fabrication of tethered polymer layers, pre-synthesized polymer chains, bearing a tethering group, are made to attach to a surface [9]. Grafting-to benefits from using polymers that can have extremely-well controlled length distribution, and does not require advanced polymer synthesis, making it a more accessible technique than grafting-from. A disadvantage of this technique lies in the fact that the polymer chains tend to deposit on the surface in their most stable (un-stretched) conformation, producing grafted layers with lower chain density than the grafting-from approach. An additional limitation is that the choice of tethering groups for effective grafting is somewhat limited. In our work, we exploited the reaction of an epoxide with a primary amine [9]. As shown in the scheme in Fig. 9(b), the system was based on a bilayer of PS and poly(lactic-*co*-glycolic acid) (PLGA). PLGA was chosen as it can be used as a safe degradable coating in physiological conditions, but has a short lifetime (of the order of several hours). PLGA films dewetted easily from PS when annealed above 120 °C, producing the expected pattern of uncorrelated circular holes. The PLGA film was then reacted by either aminolysis (with ethylenediamine) or hydrolysis (with sodium hydroxide) to introduce primary amine or hydroxide groups on the surface of the film. Poly(ethylene glycol) (PEG) bearing terminal epoxide groups was finally grafted to the amine or hydroxide groups. To maximize the density of grafted chains, the grafting was performed under cloud-point (CP) conditions, whereby the volume of the polymer chains is reduced by reducing their solubility (in our work by using 0.1 M phosphate buffer at pH 7, containing 0.8 M Na_2SO_4). The PEGylated surface grafted under CP conditions exhibited good protein resistance: fluorescence microscopy highlighted a contrast in the amount of FITC-tagged BSA adsorbed on the dewetted PEG brush, with more protein inside the holes. Quartz crystal microbalance confirmed that almost twenty times more protein adsorbed on PS compared to PLGA CP-grafted with PEG, as shown in Fig. 11 (by comparison room temperature grafting, RT, was less efficient). Interestingly, the grafted PEG layer drastically reduced the hydrolysis of PLGA. Our grafting approach slowed down the degradation of PLGA remarkably, providing both antifouling properties and tuning of the biodegradation rate of the coating.

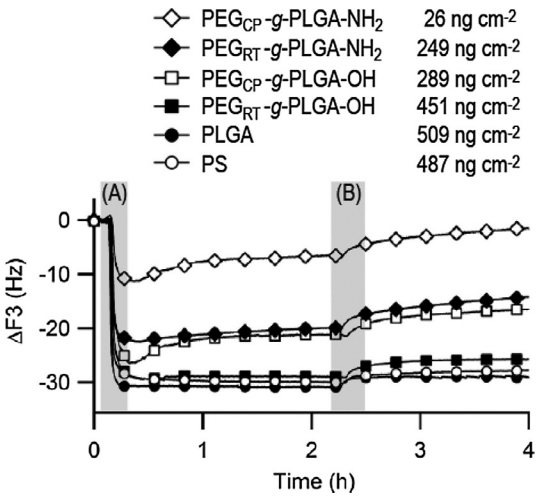

Fig. 11. Quartz crystal microbalance frequency shift (3rd harmonic) during the adsorption of BSA on tested polymer coatings. Stage (A) is when the injection of the BSA solution in PBS occurs (2 mg mL^{-1}); Stage (B) is when the rinsing with PBS occurs. The mass of the BSA adsorbed on each surface after rinsing is indicated in the legend. Reprinted with permission from Ref. [9]. Copyright 2014 American Chemical Society.

2.3. Selective attachment and patterning of cells

As discussed in Section 2.1, ECM proteins surround cells in a tissue, provide important cues that direct cell–cell interaction and contribute to the regulation of cell growth, specialization, multiplication and death, which all together maintain the normal behavior of the tissue. By patterning the appropriate ECM protein onto a surface, one can obtain a seed layer suitable for the subsequent selective attachment of cells. In our work, for example, we employed vitronectin to promote the adhesion of mouse fibroblasts, and type I collagen to pattern human umbilical vein endothelial cells. Both type of cells can interact with the seed layer of ECM proteins via specialized receptors on their outer membranes, called *integrins*, which can be thought as the cell's tactile probes to explore a surface [87]. If ECM proteins that have exposed cell-binding domains are present on the surface, the integrins will bind to them, and create tension in the cell's "skeleton" (a framework composed of the structural protein *actin*). Such mechanical input is transduced in chemical inputs within the cell, which ultimately determine its behavior [88]. Often tissue cells require spreading in order to survive. Cells that remain rounded once in contact with a surface undergo apoptosis. We studied the attachment of mouse fibroblasts onto a patterned polyPEGMA brush, and observed that cells could effectively attach inside the vitronectin-coated holes, but not on the non-fouling polymer brush around them (Fig. 12(a)) [6]. Cells spreading within the holes would depend strongly on the space available: one or two cells in wide 40 μm holes - compared to the size of a single rounded cell, approx. 15 μm - would spread to attempt to cover the entire vitronectin surface, while multiple cells would crowd together to maximize contact with both the underlying vitronectin and the neighboring cells (Fig. 12(a)). In patterns with large adhesive domains, cells had an almost 100% survival rate after 24 h, as determined by selectively staining live cells in green and dead cells in red (Fig. 12(b)). Interestingly, when the diameter of the holes was reduced to a size comparable to that of the rounded cells (20 μm), cell attachment inside the holes was no longer observed, as the adhesive domains available where too small for even minimal spreading of the fibroblasts. Only few cells could attach effectively, by bridging between two adjacent holes (see arrow in Fig. 12(c)).

As discussed in Section 2.1, cell attachment is not only influenced by the size of the adhesive domains, but also by the configuration of the seed protein layer. In PNVP dewetted patterns on top of PS, we investigated the relationship between the conformation of Collagen I on the surface and cell attachment [7]. As discussed in Section 2.1, PNVP/PS patterns provide some contrast in protein adhesion. We found that such contrast could be enhanced by treating the patterns with air plasma: the PS holes became more protein-adhesive, while the PNVP background became more protein-repellent. Interestingly, the conformation of the collagen adsorbed on the PS changed dramatically upon plasma treatment, from isolated aggregates to even "mats". The difference in collagen I conformation is evident in Fig. 13. On pristine PS (Fig. 13(a)), AFM reveals worm-like aggregates. On plasma-treated PS, AFM shows instead a much more homogeneous distribution of thinner fibrils

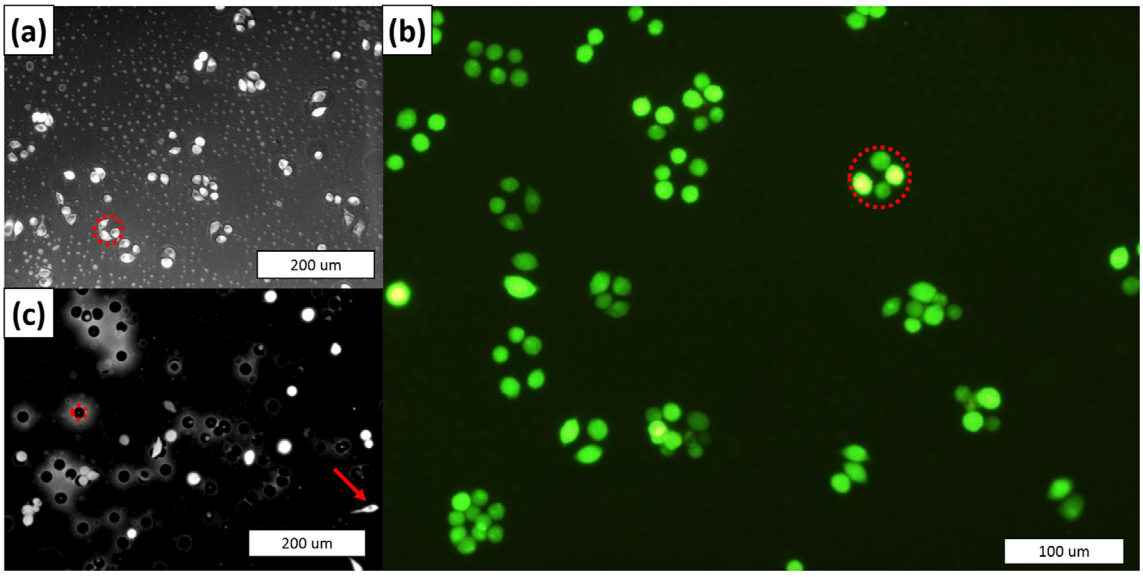

Fig. 12. Optical micrographs of mouse fibroblasts attached to dewetted polyPEGMA brushes. (a) Pattern with 40 μm dewetted holes, into which the cells could effectively attach. (b) Live-dead staining with calcein (green, live cells) and ethidium homodimer (red, dead cells): after 24 h virtually all cells observed exhibit green fluorescence. (c) Pattern with 20 μm dewetted holes, into which the cells could not attach and spread, unless bridging between two adjacent holes (red arrow). As a guide to the eye, one dewetted hole in each micrograph was highlighted in dashed red circles. (For interpretation of the references to colour in this figure legend, the reader is referred to the web version of this article.)

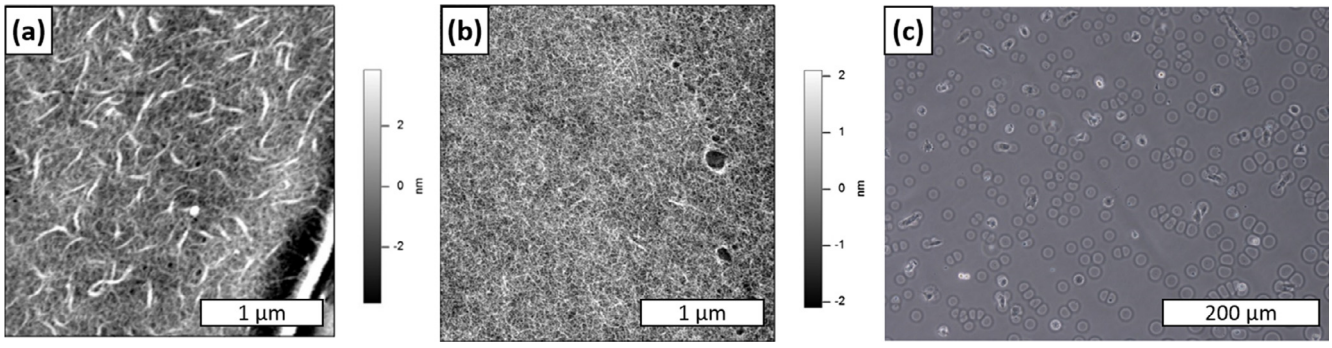

Fig. 13. Adsorption of collagen I onto PS. AFM images of collagen I onto (a) pristine PS and (b) plasma-treated PS. The conformation of collagen I changes from aggregates to a flat "mat". (c) Bright field optical micrograph of human endothelial cells attached onto a plasma-treated PNVP/PS dewetted pattern, after pre-seeding with collagen I. The cells remaining onto the surface after rinsing were bound into the dewetted holes, where the flat mats of collagen I were present. Figure (a) was adapted from Ref. [7] with permission of The Royal Society of Chemistry.

(Fig. 13(b)). The "mat" conformation provided the best substrate for the attachment of human endothelial cells, and this corresponds to common knowledge that tissue culture plates consist of plasma-treated PS. Human endothelial cells were found to attach within the protein-coated domains, and showed spreading, which is indicative of good interaction with the surface and of good viability (Fig. 13(c)). The rate of attachment was lower than that of fibroblasts in Fig. 12. As for fibroblasts, the size of the dewetted holes appeared to affect cell adhesion: larger holes provided more space for the human endothelial cells to attach [7].

3. Applications of dewetting in atmospheric water capture

A second application of patterning by dewetting that the Neto group has explored extensively over the past few years is atmospheric water capture. In light of increased occurrence of droughts, an increasing global population and growing demands on natural resources, alternative methods of water collection have received increasing attention in recent times [89]. A particularly novel approach to guaranteeing a sustainable water supply is the concept of atmospheric water harvesting – namely, taking advantage of sources of water in the air around us (e.g. humidity, fog, mist) and collecting this water via condensation on a surface, ideally with a low energetic footprint [90]. The not-for-profit organization *FogQuest* has implemented this concept in various communities throughout South and Central America (Guatemala, Chile), Asia (Nepal) as well as Africa (Morocco, Eritrea and Ethiopia) [91]. Their approach relies on the use of a high surface-area polyethylene or polypropylene mesh erected as sheets (usually 6 m high by 10 m long), typically in mountainous regions where prevailing weather patterns rely on regular foggy weather. Average collection volumes of 200 litres of water per day from a single mesh are typical – this impressive figure is of particular value for remote and rural communities where established approaches to water distribution are not possible.

In 2001, Parker and Lawrence reported the mechanism by which the Namib desert beetle could survive in one of the driest parts of Southern Africa [92]. The beetle in question is *Physosterna cripribes*, shown in Fig. 14; in nearly all publications since 2001

Fig. 14. Physosterna Cripribes (© Tracy Robb/CC BY-SA 3.0/GFDL).

(including our own) this beetle has been wrongly identified as *Stenocara dentata* or *Stenocara gracilipes* [93,94]. *Physosterna* relies on atmospheric dropwise condensation on its exoskeleton, which consists of a series of hydrophilic raised 'bumps' that are randomly distributed on a waxy background. The bumps are typically 500 μm in diameter with a separation of 500–1500 μm, whereas the waxy background was shown to exhibit a microstructure of flattened hemispheres (10 μm diameter) arranged in a hexagonal array, yielding a superhydrophobic structure. The hydrophilic domains represent nucleation points where water can preferentially condense on the surface (due to the lower barrier for droplet nucleation on hydrophilic relative to hydrophobic substrates) [95–98], however a growing droplet of water is constrained by the size of the hydrophilic spot on which it sits. As a consequence, 'pinned' water droplets will ultimately detach from the *Physosterna* exoskeleton when gravitational force becomes sufficiently large to overcome the capillary forces holding the droplet in place. This mechanism ensures that *Physosterna* obtains water to drink when exposed to fog (which consists of a dispersion of micrometre-sized water droplets in air), with the appropriate balance of size and density of hydrophilic domains to minimize re-evaporation to the atmosphere. This combination of surface chemistry and topography with respect to water-harvesting was demonstrated in simple experiments using hydrophilic (water contact angle ~20°) glass beads of 0.6 mm diameter embedded into a wax substrate (water contact angle ~110°); regular (and random) arrays of beads collected twice the volume of water than from flat glass and flat wax surfaces when exposed to a mist of water at 22 °C [92].

The identification of the water-collection mechanism of *Physosterna* has subsequently set in motion a significant body of research in the area of biomimetic surface design, towards the creation of synthetic analogues in the laboratory. Examples of some of the varied approaches towards the creation of surface coatings that promote drop-wise condensation in a manner similar to that seen in nature are summarized in Table 1. The design rules are relatively straightforward: a (super)hydrophobic base layer, with raised hydrophilic domains distributed across the surface (in the micrometre to millimetre size range) [99]. Such surfaces can be readily achieved via the dewetting of polymer bilayers, where a hydrophilic top layer dewets from a hydrophobic underlayer, as has been demonstrated by the Neto group [5,13,100]. We believe that the dewetting approach realizes several technical advantages compared to other approaches listed in Table 1, the main ones being simplicity and scalability. In addition, the rise in functional polymeric materials via 'living' polymerization techniques [101], in addition to post-polymerization modification [102], we believe offers additional scope and utility to the dewetting process for the continual realization of new micro-patterned substrates.

Table 1
Summary of methods to replicate the surface structure of the *Physosterna* beetle.

Method	Reference(s)
Dewetting of polymer films (thermal or solvent annealing)	Thickett et al. [5] Wong et al. [100] Al-Khayat et al. [13]
Manual deposition onto superhydrophobic surfaces	Zhai et al. [103]
Plasma-chemical treatment	Dorrer et al. [104] Garrod et al. [105]
Lithography	Lee et al. [106]
Computer-aided Design	Ghosh et al. [107]
Chemical Vapor Deposition	Kim et al. [108]
Hexagonal 'cactus inspired' cone arrays	Ju et al. [109]
3D Printing	Zhang et al. [110]
Janus-materials	Cao et al. [111,112]
Patterned 1D fibres	Hou et al. [113]
Hydrophobized metal nanowires	Wen et al. [114]
Surface-modification of various meshes (metal and polymeric)	Zhu et al. [115] Rajaram et al. [116] Wang et al. [117]
Metallic foams	Ji et al. [118]

3.1. Atmospheric water collection studies on dewetted surfaces via thermal annealing

When optimized for the creation of isolated poly(4-vynylpyridine) (P4VP) domains on a background of polystyrene (PS), micropatterned substrates prepared via thermal annealing and dewetting proved to be efficient dropwise condensers for atmospheric water [5]. The approach adopted in the Neto group was to study condensation directly from humidified air (RH ranging from 50 to 80%), as opposed to exposing surfaces to a preformed fog or mist (RH ~ 100%). Time-lapse optical microscopy of patterned surfaces on a Peltier cooling plate (cooled at a temperature ΔT = 10 K below the dew point under ambient conditions, i.e. no moving air) was used to verify the drop-wise condensation mechanism. Condensation takes place on all surfaces, with small rounded water droplets on the hydrophobic PS and large flattened droplets on the hydrophilic P4VP; on the dewetted surfaces, water droplets nucleated preferably on the hydrophilic P4VP domains rather than on the PS background (Fig. 15). Water droplets were shown to grow in volume upon continual exposure to humid air, often coalescing with neighboring water droplets and being pinned by several P4VP domains at a time (Fig. 15(C)). Droplet coalescence was due to the very small P4VP domain size (typically 7–12 μm) formed via thermal annealing, approximately two orders of magnitude smaller than that seen on the *Physosterna* beetle. The ability to tune hydrophilic domain size is addressed in further detail later in this Section, however dewetted substrates do indeed display dropwise condensing behavior.

Macroscopic studies related to the rate of water condensation and droplet detachment also demonstrated a benefit of preparing micro-patterned substrates with respect to their flat counterparts. Upon exposure to a flow of humid air mimicking a wind speed of ~10 km h^{-1}, patterned surfaces cooled 10 K below the dew point could collect ~3.4 L m^{-2} h^{-1}, representing a nearly 40% increase in condensation efficiency with respect to a flat hydrophilic P4VP film. The critical volume for droplet detachment V_{crit} from a tilted substrate was measured to be ~15 μL for the P4VP/PS micropatterned surfaces, whereas water droplets did not detach from a flat P4VP surface until well over 35 μL in volume.

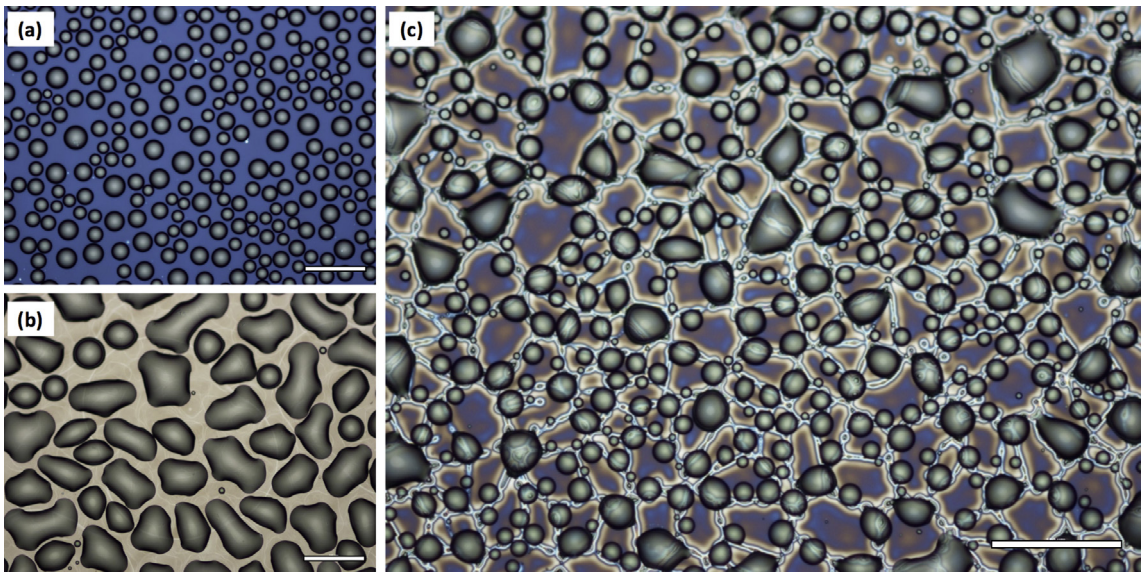

Fig. 15. Optical micrographs highlighting condensation of water on (a) flat PS; (b) flat P4VP and (c) dewetted PV4 P on PS polymer films prepared via thermal annealing at 200 °C for 5 min. Images were taken after 5 min of cooling 10 K below the dew point on a Peltier plate. In panel (c), nucleated water droplets can be seen on individual P4VP domains or pinned across multiple P4VP sites. All scale bars = 100 μm.

The static water contact angle for the dewetted surfaces was similar to the background PS phase (PS = 91°, dewetted substrate = 90°), whereas the dynamic contact angle behavior was intermediate between that of PS and P4VP. Importantly, the contact angle hysteresis of the dewetted substrate was 10° lower than the flat P4VP film (from ~33° to ~23°), a property that aids water droplet detachment at smaller volumes [119]. Analogous to *Physosterna*, rapid water droplet detachment frees up the surface for further condensation, increasing the rate of condensation overall.

Our initial work in this area was performed with commercial polymer standards, typically prepared via anionic polymerization. The rise of reversible deactivation radical polymerization (RDRP) techniques over the past two decades has revolutionized the ability to prepare polymers with low dispersity and targeted average molecular weight, using non-stringent reaction conditions compared to anionic methods. Techniques such as reversible addition fragmentation chain-transfer (RAFT) [120–122], atom transfer radical polymerization (ATRP) [123] and nitroxide-mediated radical polymerization (NMP) [124] enable the controlled polymerization of most common classes of monomers; the resulting polymers carry an active chain end that allows for subsequent chain growth and (potentially) the formation of block copolymers in a controlled fashion. RDRP techniques also enable the creation of controlled polymer brush surfaces, as outlined in Section 2.2. Given the influence of polymer molecular weight on melt viscosity and hole nucleation density discussed earlier, the ability to target a defined polymer molecular weight with low dispersity is ideal for both fundamental and applied dewetting research. RDRP-based techniques therefore offer a simple route to controlling microstructure composition.

We have recently utilized RAFT polymerization for the design of a hydrophilic, water-insoluble polymer, poly(2-hydroxypropyl methacrylate) (PHPMA), used for the first time for the creation of water-condensing surfaces [100]. PHPMA is one of the most suitable polymers for the hydrophilic 'top' layer of a bilayer system for thin film dewetting, given its physical properties: it is glassy at room temperature (T_g ~ 84–103 °C [100,125]), is moderately hydrophilic (equilibrium contact angle ~57° for high molecular weight samples) and is immiscible with hydrophobic polymers such as PS. Three PHPMA samples of low dispersity (Đ < 1.3) and varying molecular weight (M_n ranging from 9.6 to 80 kDa) were prepared in order to examine the role of molecular weight in the dewetting of PHPMA/PS bilayers prepared via spin coating. Highlighting the importance of molecular weight, the 9.6 kDa PHPMA sample exhibited spontaneous partial dewetting (known as 'spin dewetting' [126,127]) upon spin-coating on top of a PS thin film. The low molecular weight of this polymer coupled with its casting as a thin film (~35 nm) has the effect of drastically reducing the effective T_g [128], in this case lowering the T_g of PHPMA below room temperature and hence promoting the spontaneous dewetting process. Higher molecular weight PHPMA samples produced stable bilayer films when cast on top of PS; thermal annealing of these bilayers at temperatures greater than 130 °C yielded dewetted substrates via heterogeneous nucleation that could proceed to a completely dewetted surface. Once more, significant molecular weight effects on dewetted surface morphology were seen – there was a near 5-fold increase in hydrophilic 'bump' density for 80 kDa PHPMA substrates compared to 18 kDa PHPMA, in line with previous reports [35]. The 80 kDa PHPMA sample also demonstrated a combination of PHPMA droplets connected via interconnected cylindrical domains, whereas the lower molecular weight could form fully isolated droplets (Fig. 16). In a manner analogous to our previously reported P4VP/PS substrates, these coatings were efficient drop-wise condensing surfaces when cooled and exposed to humid air (55% RH, cooled ΔT = 2 K below the dew point) with a significant reduction in contact angle hysteresis with respect to flat hydrophilic PHPMA films.

3.2. Effect of pattern size on water capture efficiency

Thermal annealing of polymer bilayers to induce dewetting suffers from an inherent limitation with respect to the pattern size (hydrophilic bump height and diameter) and density for the design of surfaces for water condensation studies. Thermally annealed polymer bilayers typically produce hydrophilic patterns where the bump diameter is of the order of 7–12 μm with bump heights no greater than 2 μm, due to the low thickness of the films (typically around or below 100 nm), and the obtainable droplet density is similarly limited.

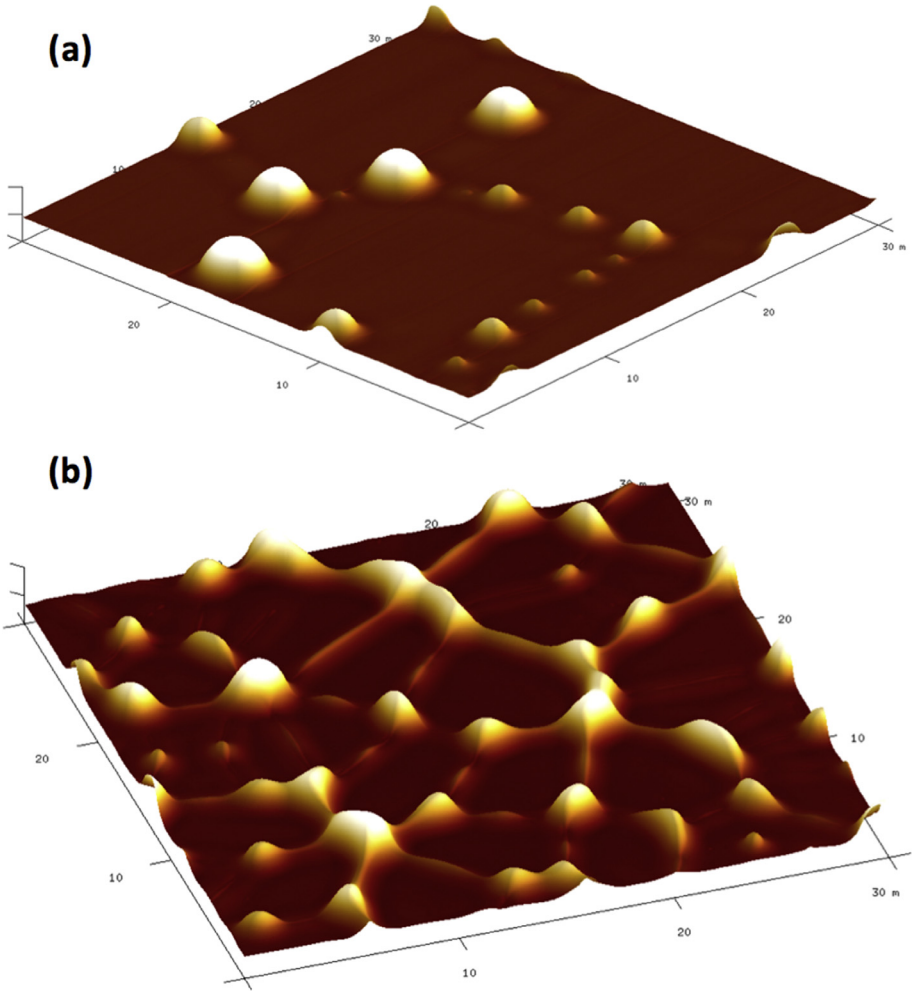

Fig. 16. Influence of PHPMA molecular weight on surface morphology via thermal annealing: 3D AFM topographical images of (a) 18 kDa PHPMA on PS and (b) 80 kDa PHPMA on PS. The higher molecular weight PHPMA film consists of interconnected domains and cylinders of polymer. Both images have lateral dimensions of 30 μm × 30 μm; in panel (a) the height is 1000 nm, in panel (b) the height is 750 nm.

To overcome these limitations, the Neto group has recently turned to solvent vapor annealing in order to achieve surface patterns of vastly different size and density for water collection studies, as mentioned in Section 1.4 [11,12]. The polymer bilayers were exposed to a saturated mixture of solvent vapor in a closed system at a fixed temperature. From a surface preparation perspective, this enabled the design of fully dewetted P4VP droplets on a PS background with essentially no layer inversion or interconnected cylindrical domains, which are typical features of thermally annealed bilayers. Using optimized solvent vapor annealing conditions for P4VP/PS bilayers (70:30 w/w acetone–water as annealing solvent), dewetted P4VP droplets with an average diameter ranging from < 1 μm through to over 80 μm have been successfully prepared (Fig. 17) [12]. Coupled to this size increase, the average height of isolated P4VP droplets varied from 44 nm through to 10 μm, with the droplet density varying by over four orders of magnitude. This was achieved by simply altering the initial P4VP film thickness (from 7 nm for the smallest droplets prepared, through to 820 nm for the largest droplets; the PS underlayer was ~110 nm thick in all cases). Further demonstrating the utility of the dewetting concept, these films were prepared by dip-coating onto either flat copper sheets or 10 mm diameter copper tubing, highlighting the ability to pattern non-planar substrates. Flat hydrophilic, flat hydrophobic and patterned substrates were then studied with respect to surface coverage (and volume) of condensed water at different cooling levels below the dew point ($2\ K \leq \Delta T \leq 5\ K$). Due to the low water contact angle of flat P4VP films, these surfaces always had greater surface water coverage than flat hydrophobic films, regardless of the level of cooling. However, if the level of cooling was too high ($\Delta T = 5$ K, 85%RH), all surfaces (flat and patterned) behaved comparably due to the similar macroscopic wettability of the substrates and similar energetic barriers to water nucleation [13].

The importance of both surface cooling and pattern size was evaluated. Similar to the experiments discussed above, if there was plenty of water in the atmosphere surrounding the surfaces (high cooling or high humidity), all substrates collected essentially the same amount of water. The influence of pattern size was most influential when the barrier for nucleation was high, for example when the surface was only slightly cooled below atmospheric temperature (cooling $\Delta T = 3$ K, at 95%RH); the 'macro-pattern' (with P4VP domains ~80 μm diameter) collected the most water of any patterned surface (14.5 ± 1.1 mL m^{-2} h^{-1} across a 6 h period), and was 57% more effective than a flat hydrophobic PS coating. The size of the hydrophilic domains in the macro-pattern was critical in supporting growth of nucleated water droplets until detachment; condensation on surfaces with smaller patterned features resulted in coalescence of neighboring water droplets, resulting in greater contact line pinning. A higher level of cooling naturally increased the overall water condensation rate on all surfaces,

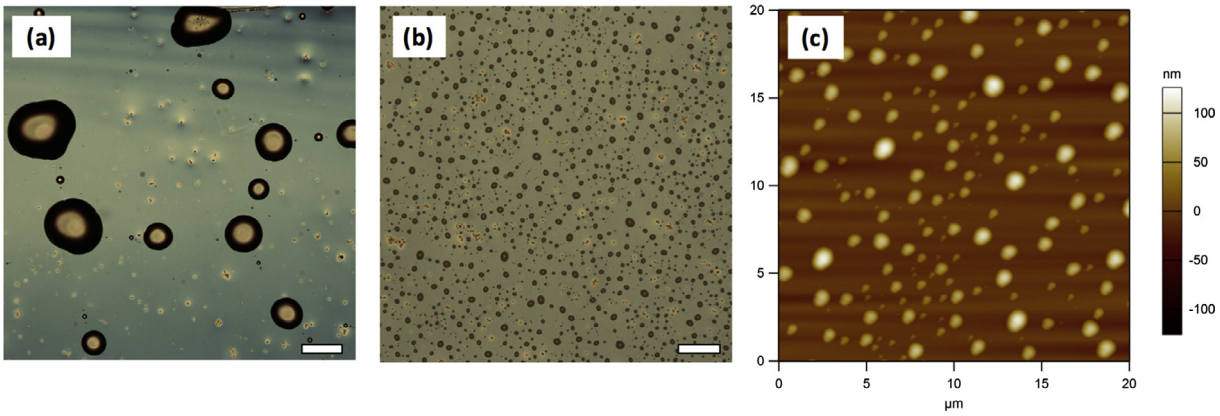

Fig. 17. Preparation of polymeric patterns of different sizes via solvent annealing of P4VP (of varying film thickness) from a PS underlayer. The annealing solvent was a 70:30 acetone:water w/w mixture in all cases. Left to right: Optical micrographs of (a) "macro" patterns and (b) "micro" patterns (scale bar = 200 μm in both cases); c) AFM topography image of a "nano" pattern.

however the benefit of any patterning was lost when the amount of water present was high. Importantly, low levels of cooling can be easily achieved under passive conditions, i.e. upon radiative cooling of surfaces at night time [129]; this demonstrates the ability to facilitate enhanced drop-wise condensation using surfaces prepared by solvent annealing.

4. Conclusions and outlook

The requirement for chemically and/or topographically heterogeneous surfaces is ubiquitous in many technology industries, including (but not limited to) medical devices, custom coatings for pipes and vessels in chemical plants, optics, paints, research laboratories, and microelectronics. The techniques developed to fabricate such heterogeneous surfaces are many and varied, and the choice of the appropriate one depends on four main requirements: cost, scalability, feature resolution and pattern geometry (or order). For example, photolithography can achieve high resolution and lateral order in a pattern, but it is relatively expensive and limited in scale. It is ideal for the microelectronics industry, but poorly suited for large area outdoor coatings. Patterning by dewetting instead, is a remarkable solution in applications where low cost and scalability are the main requirements. Such applications include biomedical devices and water capture devices, which we have discussed in detail in this Article.

As discussed in Section 1.1, some of the limitations of using dewetting for patterning have been recently addressed. Order can be induced in the patterns by the use of pre-patterning strategies, for example by self-assembling a monolayer of particles on top of a polymer film, and embossing the film by careful annealing. Work is still in progress to develop more and better pre-patterning methods based on self-assembly, which can retain the advantages of low-cost, scalability and simplicity. In terms of pattern dimensions, progress has been made on extending the range of feature diameter and height in dewetted patterns. The solvent annealing approach has allowed to pattern coatings as thick as a few micrometers, instead of a couple of hundred nanometers. Thicker coatings are more mechanically stable, improving the potential for practical applications. Maintaining a narrow dispersity in the range of lateral dimensions (width of the features), is more complex and effective strategies are still under investigation.

The future of research on patterning by dewetting is particularly exciting, thanks to the potential developments of this technique related to its dual nature. On one hand, patterning by dewetting is low cost and can be developed using simple facilities; furthermore, thanks to the large body of fundamental and applied work published by various academic groups, including the Neto group, it can be used simply as a tool, not requiring in-depth knowledge of intermolecular forces or thin film dynamics. This implies that further applications can be developed anywhere in the world, including countries where specialized and technical facilities are hard to access. On the other hand, patterning by dewetting can reach a high level of sophistication, as described in some of the examples in this Article. Recent advances in polymer synthesis and in colloid self-assembly have immediate benefits for patterning by dewetting, such as fine control of surface chemistry and mechanical properties (for example with polymer brushes or tailored polymers in the top layer), and control over the pattern geometry, without sacrificing the low cost and scalability of the technique.

In conclusion, patterning by dewetting is a remarkable example of how fundamental understanding of physical phenomena can lead to useful technology, especially when it is approached with a multidisciplinary mindset.

Acknowledgements

The authors thank Dr. Omar Al-Khayat, Dr. Manuel Ghezzi and Mr. Ming Chiu for contributing some of the presented images.

References

[1] W. Han, Z.Q. Lin, Learning from "Coffee Rings": ordered structures enabled by controlled evaporative self-assembly, Angew. Chem.-Int. Ed. 51 (7) (2012) 1534–1546.
[2] A. Munoz-Bonilla, M. Fernandez-Garcia, J. Rodriguez-Hernandez, Towards hierarchically ordered functional porous polymeric surfaces prepared by the breath figures approach, Prog. Polym. Sci. 39 (3) (2014) 510–554.
[3] C. Neto, A novel approach to the micropatterning of proteins using dewetting of polymer bilayers, Phys. Chem. Chem. Phys. 9 (2007) 149–155.
[4] S.C. Thickett, A. Harris, C. Neto, Interplay between dewetting and layer inversion in poly(4-vinylpyridine)/polystyrene bilayers, Langmuir 26 (20) (2010) 15989–15999.
[5] S.C. Thickett, C. Neto, A.T. Harris, Biomimetic surface coatings for atmospheric water capture prepared by dewetting of polymer films, Adv. Mat. 23 (32) (2011) 3718–3722.
[6] A.M. Telford et al., Micro-patterning of polymer brushes: grafting from dewetting polymer films for biological applications, Biomacromol 13 (9) (2012) 2989–2996.
[7] S.C. Thickett et al., Micropatterned substrates made by polymer bilayer dewetting and collagen nanoscale assembly support endothelial cell adhesion, Soft Matter 8 (2012) 9996–10007.
[8] A.M. Telford, C. Neto, L. Meagher, Robust grafting of PEG-methacrylate brushes from polymeric coatings, Polymer 54 (2013) 5490–5498.
[9] M. Ghezzi et al., Protein micro-patterns by PEG grafting on dewetted PLGA films, Langmuir 30 (2014) 11714–11722.
[10] M. Ghezzi et al., Guiding the dewetting of thin polymer films by colloidal imprinting, Adv. Mater. Interfaces 2 (11) (2015) 1500068.

[11] O. Al-Khayat et al., Chain collapse and interfacial slip of polystyrene films in good/nonsolvent vapor mixtures, Macromolecules 49 (2016) 1344–1352.
[12] O. Al-Khayat et al., 'The Good, the Bad and the Slippery': a tale of three solvents in polymer film dewetting, Macromolecules 49 (17) (2016) 6590–6598.
[13] O. Al-Khayat et al., Patterned polymer coatings increase the efficiency of dew harvesting, ACS Appl. Mater. Interfaces (2017), http://dx.doi.org/10.1021/acsami.6b16248.
[14] F. Brochard-Wyart, P.G. de Gennes, Shear-dependent slippage at a polymer/solid interface, Langmuir 8 (1992) 3033–3037.
[15] F. Brochard-Wyart, P.G. de Gennes, Dynamics of partial wetting, Adv. Colloid Interface Sci. 39 (1992) 1–11.
[16] F. Brochard-Wyart et al., Spreading of nonvolatile liquids in a continuum picture, Langmuir 7 (1991) 335–338.
[17] P.G. de Gennes, Wetting: statics and dynamics, Rev. Mod. Phys. 57 (1985) 827.
[18] P.G. de Gennes, Polymers at an interface; a simplified view, Adv. Colloid Interface Sci. 27 (1987) 189–209.
[19] P.-G. de Gennes, F. Brochard-Wyart, D. Quéré, Capillarity and Wetting phenomena. Drops, Bubbles, Pearls, Waves, Springer, New York, 2004.
[20] D. Quere, Wetting and Roughness, Ann. Rev. Mater. Res. 38 (1) (2008) 71.
[21] D. Quéré, Non-sticking drops, Rep. Prog. Phys. 68 (2005) 2495–2532.
[22] D. Quéré, Wetting and Roughness, Ann. Rev. Mater. Res. 38 (1) (2008) 71–99.
[23] G. Reiter, Dewetting of Thin Polymer Films, Phys. Rev. Lett. 68 (1) (1992) 75–78.
[24] H. Gau et al., Liquid morphologies on structured surfaces: from microchannels to microchips, Science 283 (1999) 46–49.
[25] S. Herminghaus et al., Spinodal dewetting in liquid crystal and liquid metal films, Science 282 (916–919) (1998).
[26] K. Jacobs, S. Herminghaus, K.R. Mecke, Thin liquid polymer films rupture via defects, Langmuir 14 (1998) 965–969.
[27] R. Seemann et al., Dynamics and structure formation in thin polymer melt films, J. Phys.: Condens. Matter 17 (2005) S267–S290.
[28] J. Becker et al., Complex dewetting scenarios captures by thin film models, Nat. Mater. 2 (2003) 59–63.
[29] R. Seemann, S. Herminghaus, K. Jacobs, Dewetting patterns and molecular forces: a reconciliation, Phys. Rev. Lett. 86 (24) (2001) 5534–5537.
[30] R. Fetzer et al., New slip regimes and the shape of dewetting thin liquid films, Phys. Rev. Lett. 95 (2005) 127801.
[31] B. Oliver et al., Slippage and nanorheology of thin liquid polymer films, J. Phys.: Condens. Matter 24 (32) (2012) 325102.
[32] S. Haefner et al., Influence of slip on the Plateau-Rayleigh instability on a fibre, Nat. Commun. 6 (2015).
[33] S. Al Akhrass et al., Viscoelastic thin polymer films under transient residual stresses: two-stage dewetting on soft substrates, Phys. Rev. Lett. 100 (17) (2008) 178301.
[34] P. Damman et al., Relaxation of residual stress and reentanglement of polymers in spin-coated films, Phys. Rev. Lett. 99 (3) (2007) 036101.
[35] G. Reiter et al., Residual stresses in thin polymer films cause rupture and dominate early stages of dewetting, Nat. Mater. 4 (2005) 754–758.
[36] R. Xie et al., Spinodal dewetting of thin polymer films, Phys. Rev. Lett. 81 (6) (1998) 1251–1254.
[37] S. Herminghaus, R. Seeman, K. Jacobs, Generic morphologies of viscoelastic dewetting fronts, Phys. Rev. Lett. 89 (5) (2002) 56101.
[38] G. Reiter, P. Auroy, L. Auvray, Instabilities of thin polymer films on layers of chemically identical grafted molecules, Macromolecules 29 (1996) 2150–2157.
[39] G. Reiter, R. Khanna, Real-time determination of the slippage length in autophobic polymer dewetting, Phys. Rev. Lett. 85 (2000) 2753–2756.
[40] G. Reiter, Evolution of rim instabilities in the dewetting of slipping thin polymer films, J. Adhesion 81 (3–4) (2005) 381–395.
[41] O. Bäumchen et al., Influence of slip on the rayleigh-plateau rim instability in dewetting viscous films, Phys. Rev. Lett. 113 (1) (2014) 014501.
[42] J.D. McGraw et al., Nanofluidics of thin polymer films: Linking the slip boundary condition at solid–liquid interfaces to macroscopic pattern formation and microscopic interfacial properties, Adv. Coll. Interface. Sci. 210 (2014) 13–20.
[43] C. Neto, Effect of Chain length on the fingering instability in dewetting Polymer Films. (2017) (submitted for publication).
[44] F. Brochard Wyart, J. Daillant, Drying of solids wetted by thin liquid films, Can. J. Phys. 68 (1990) 1084–1088.
[45] C. Neto, K. Jacobs, Dynamics of hole growth in dewetting polystyrene films, Phys. A 339 (1–2) (2004) 66–71.
[46] F. Brochard Wyart, P. Martin, C. Redon, Liquid/liquid dewetting, Langmuir 9 (1993) 3682–3690.
[47] G. Krausch, Dewetting at the interface between two immiscible polymers, J. Phys.: Condens. Matter 9 (1997) 7741–7752.
[48] R. Fetzer, K. Jacobs, Slippage of Newtonian liquids: influence on the dynamics of dewetting thin films, Langmuir 23 (23) (2007) 11617–11622.
[49] C. Wang, G. Krausch, M. Geoghegan, Dewetting at a polymer-polymer interface: film thickness dependence, Langmuir 17 (2001) 6269–6274.
[50] P. Damman, N. Baudelet, G. Reiter, Dewetting near the glass transition: transition from a capillary force dominated to a dissipation dominated regime, Phys. Rev. Lett. 91 (21) (2003) 216101.
[51] T. Vilmin et al., The role of nonlinear friction in the dewetting of thin polymer films, Europhys. Lett. 73 (2006) 906–912.
[52] F. Brochard-Wyart et al., Dewetting of supported viscoelastic polymer films: birth of rims, Macromolecules 30 (1997) 1211–1213.
[53] H. Lee et al., Autophobic dewetting of polystyrenes on the substrates grafted with chemically identical polymers, Polym. J. 48 (4) (2016) 503–507.
[54] G. Reiter, R. Khanna, Kinetics of autophobic dewetting of polymer films, Langmuir 16 (15) (2000) 6351–6357.
[55] M. Cavallini et al., Conformational self-recognition as the origin of dewetting in bistable molecular surfaces, J. Phys. Chem. B 105 (44) (2001) 10826–10830.
[56] J. Brandrup, E.H. Immergut, Polymer Handbook, Third ed., John Wiley and Sons, Inc., 1989.
[57] M. Rowe et al., High Glass transition temperature fluoropolymers for hydrophobic surface coatings via RAFT copolymerization, Austr. J. Chem. 69 (2016) 725–734.
[58] P.G. de Gennes, Reptation of a polymer chain in the presence of fixed obstacles, J. Chem. Phys. 55 (2) (1971) 572–579.
[59] J. Des Cloizeaux, Polymer melt: reptation of a chain and viscosity, J. Phys. Lett. 45 (1984) 17–26.
[60] M. Doi, S.F. Edwards, Dynamics of concentrated polymer systems. Part 1. – brownian motion in the equilibrium state, J. Chem. Soc. Faraday Trans. 2: Molecular Chem. Phys 74 (1978) 1789–1801.
[61] C.C. Li et al., Melt fracture in polymer thin films at strongly attractive surfaces, Europhys. Lett. 76 (2006) 870–876.
[62] P.G. de Gennes, Wetting: statics and dynamics, Rev. Mod. Phys. 57 (3) (1985) 827.
[63] G. Reiter, Dewetting of highly elastic thin polymer films, Phys. Rev. Lett. 87 (2001) 186101.
[64] A. Sharma, R. Khanna, Pattern formation in unstable thin liquid films, Phys. Rev. Lett. 81 (16) (1998) 3463–3466.
[65] A. Shultz, P. Flory, Polymer chain dimensions in mixed-solvent media, J. Polym. Sci. 15 (79) (1955) 231.
[66] J. Magda et al., Dimensions of a polymer chain in a mixed solvent, Macromolecules 21 (3) (1988) 726–732.
[67] A.R. Khokhlov, A.Y. Grosberg, V.S. Pande, Statistical Physics of Macromolecules, Springer, 1994.
[68] M. Nakata, Coil-globule transition of poly(methyl methacrylate) in a mixed solvent, Phys. Rev. E 51 (6) (1995) 5770.
[69] P. Auroy, L. Auvray, Collapse-stretching transition for polymer brushes: preferential solvation, Macromolecules 25 (16) (1992) 4134–4141.
[70] D. Gentili et al., Applications of dewetting in micro and nanotechnology, Chem. Soc. Rev. 41 (12) (2012) 4430–4443.
[71] M. Ghezzi, S.C. Thickett, C. Neto, Early and intermediate stages of guided dewetting in polystyrene thin films, Langmuir 28 (27) (2012) 10147–10151.
[72] K. von der Mark et al., Nanoscale engineering of biomimetic surfaces: cues from the extracellular matrix, Cell Tissue Res. 339 (1) (2009) 131.
[73] J. El-Ali, P.K. Sorger, K.F. Jensen, Cells on chips, Nature 442 (7101) (2006) 403–411.
[74] D. Falconnet et al., Surface engineering approaches to micropattern surfaces for cell-based assays, Biomaterials 27 (16) (2006) 3044–3063.
[75] X. Xu, M.C. Farach-Carson, X. Jia, Three-dimensional in vitro tumor models for cancer research and drug evaluation, Biotechnol. Adv. 32 (7) (2014) 1256–1268.
[76] S. Talukdar et al., Effect of initial cell seeding density on 3D-engineered silk fibroin scaffolds for articular cartilage tissue engineering, Biomaterials 32 (34) (2011) 8927–8937.
[77] C.A. Goubko, X. Cao, Patterning multiple cell types in co-cultures: A review, Mater. Sci. Eng., C 29 (6) (2009) 1855–1868.
[78] H. Kaji et al., Engineering systems for the generation of patterned co-cultures for controlling cell–cell interactions, Biochim. Biophys. Acta (BBA) – General Subjects 1810 (3) (2011) 239–250.
[79] L. Yu, L. Zhang, Y. Sun, Protein behavior at surfaces: Orientation, conformational transitions and transport, J. Chromatogr. A 1382 (2015) 118–134.
[80] S. Chen et al., Surface hydration: principles and applications toward low-fouling/nonfouling biomaterials, Polymer 51 (23) (2010) 5283–5293.
[81] A.M. Telford et al., Thermally cross-linked PNVP films as antifouling coatings for biomedical applications, ACS Appl. Mater. Interfaces. 2 (8) (2010) 2399–2408.
[82] D.G. Castner, B.D. Ratner, Biomedical surface science: foundations to frontiers, Surf. Sci. 500 (2002) 28–60.
[83] J. Rühe, Polymer brushes: on the way to tailor-made surfaces, in: Polymer Brushes, Wiley-VCH Verlag GmbH & Co. KGaA, 2005, pp. 1–31.
[84] E.P.K. Currie, W. Norde, M.A. Cohen Stuart, Tethered polymer chains: surface chemistry and their impact on colloidal and surface properties, Adv. Coll. Interface. Sci. 100–102 (2003) 205–265.
[85] J.O. Zoppe et al., Surface-initiated controlled radical polymerization: state-of-the-art, opportunities, and challenges in surface and interface engineering with polymer brushes, Chem. Rev. 117 (3) (2017) 1105–1318.
[86] W.A. Braunecker, K. Matyjaszewski, Controlled/living radical polymerization: Features, developments, and perspectives, Prog. Polym. Sci. 32 (1) (2007) 93–146.
[87] C.S. Chen et al., Geometric control of cell life and death, Science 276 (1997) 1425–1428.
[88] Z. Sun, S.S. Guo, R. Fässler, Integrin-mediated mechanotransduction, J. Cell Biol. 215 (4) (2016) 445–456.
[89] M.M. Mekonnen, A.Y. Hoekstra, Four billion people facing severe water scarcity, Sci. Adv. 2 (2) (2016).

[90] G. Vince, Out of the Mist, Science 330 (2010) 750–751.
[91] FogQuest. [Accessed April 6, 2017]; Available from: http://www.fogquest.org.
[92] A.R. Parker, C.R. Lawrence, Water capture by a desert beetle, Nature 414 (2001) 33–34.
[93] F.T. Malik et al., Nature's moisture harvesters: a comparative review, Bioinspir Biomim 9 (3) (2014) 031002.
[94] T. Nørgaard, M. Dacke, Fog-basking behaviour and water collection efficiency in Namib Desert Darkling beetles, Front. Zool. 7 (1) (2010) 1–8.
[95] D. Beysens, Dew nucleation and growth, C. R. Phys. 7 (9–10) (2006) 1082–1100.
[96] M. Volmer, A. Weber, Nucleus formation in supersaturated systems, Z. Physik. Chem. 119 (1926) 277–301.
[97] K.K. Varanasi et al., Spatial control in the heterogeneous nucleation of water, Appl. Phys. Lett. 95 (9) (2009) 094101–094103.
[98] K.K. Varanasi, D. Tao, Controlling nucleation and growth of water using hybrid hydrophobic-hydrophilic surfaces, in: 2010 12th IEEE Intersociety Conference on Thermal and Thermomechanical Phenomena in Electronic Systems (ITherm), 2010.
[99] C. Graham, P. Griffith, Drop size distributions and heat transfer in dropwise condensation, Int. J. Heat. Mass. Transfer 16 (2) (1973) 337–346.
[100] I. Wong et al., Micropatterned surfaces for atmospheric water condensation via controlled radical polymerization and thin film dewetting, ACS Appl. Mater. Interfaces. 7 (38) (2015) 21562–21570.
[101] R.F. Storey, CHAPTER 2 Fundamental aspects of living polymerization, in: Fundamentals of Controlled/Living Radical Polymerization, The Royal Society of Chemistry, 2013, pp. 60–77.
[102] H. Jo, P. Theato, Post-polymerization modification of surface-bound polymers, in: P. Vana (Ed.), Controlled Radical Polymerization at and from Solid Surfaces, Springer International Publishing, Cham, 2016, pp. 163–192.
[103] L. Zhai et al., Patterned superhydrophobic surfaces; toward a synthetic mimic of the namib desert beetle, Nano Lett. 6 (6) (2006) 1213–1217.
[104] C. Dorrer, J. Ruehe, Mimicking the stenocara beetle – dewetting of drops from a patterned superhydrophobic surface, Langmuir 24 (2008) 6154–6158.
[105] R.P. Garrod et al., Mimicking a stenocara beetle's back for microcondensation using plasmachemical patterned superhydrophobic-superhydrophilic surfaces, Langmuir 23 (2) (2007) 689–693.
[106] S. Lee et al., Continuous fabrication of bio-inspired water collecting surface via roll-type photolithography, Int. J. Precis. Eng. Manuf.-Green Technol. 1 (2) (2014) 119–124.
[107] A. Ghosh et al., Enhancing dropwise condensation through bioinspired wettability patterning, Langmuir 30 (43) (2014) 13103–13115.
[108] G.-T. Kim et al., Wetting-transparent graphene films for hydrophobic water-harvesting surfaces, Adv. Mater. 26 (30) (2014) 5166–5172.
[109] J. Ju et al., Cactus stem inspired cone-arrayed surfaces for efficient fog collection, Adv. Func. Mater. 24 (44) (2014) 6933–6938.
[110] L. Zhang et al., Inkjet printing for direct micropatterning of a superhydrophobic surface: toward biomimetic fog harvesting surfaces, J. Mater. Chem. A 3 (6) (2015) 2844–2852.
[111] M. Cao et al., Facile and large-scale fabrication of a cactus-inspired continuous fog collector, Adv. Funct. Mater. 24 (21) (2014) 3235–3240.
[112] M. Cao et al., Hydrophobic/hydrophilic cooperative janus system for enhancement of fog collection, Small (2015), http://dx.doi.org/10.1002/smll.201500647.
[113] Y. Hou et al., Temperature-triggered directional motion of tiny water droplets on bioinspired fibers in humidity, Chem. Commun. 49 (46) (2013) 5253–5255.
[114] R. Wen et al., Hydrophobic copper nanowires for enhancing condensation heat transfer, Nano Energy 33 (2017) 177–183.
[115] H. Zhu et al., High-efficiency water collection on biomimetic material with superwettable patterns, Chem. Commun. 52 (84) (2016) 12415–12417.
[116] M. Rajaram et al., Enhancement of fog-collection efficiency of a Raschel mesh using surface coatings and local geometric changes, Colloids Surf., A 508 (2016) 218–229.
[117] Y. Wang et al., A facile strategy for the fabrication of a bioinspired hydrophilic-superhydrophobic patterned surface for highly efficient fog-harvesting, J. Mater. Chem. A 3 (37) (2015) 18963–18969.
[118] K. Ji et al., Centrifugation-assisted fog-collecting abilities of metal-foam structures with different surface wettabilities, ACS Appl. Mater. Interfaces. 8 (15) (2016) 10005–10013.
[119] C.G.L. Furmidge, Studies at phase interfaces. I. The sliding of liquid drops on solid surfaces and a theory for spray retention, J. Colloid Sci. 17 (4) (1962) 309–324.
[120] G. Moad, E. Rizzardo, S.H. Thang, Radical addition-fragmentation chemistry in polymer synthesis, Polymer 49 (5) (2008) 1079–1131.
[121] G. Moad et al., Advances in RAFT polymerization: the synthesis of polymers with defined end-groups, Polymer 46 (2005) 8458–8468.
[122] J. Chiefari et al., Living Free-radical polymerization by reversible addition-fragmentation chain transfer: The RAFT process, Macromolecules 31 (1998) 5559–5562.
[123] K. Matyjaszewski, N.V. Tsarevsky, Macromolecular engineering by atom transfer radical polymerization, J. Am. Chem. Soc. 136 (18) (2014) 6513–6533.
[124] J. Nicolas et al., Nitroxide-mediated polymerization, Progr. Polym. Sci. 38 (1) (2013) 63–235.
[125] P.M. Kou et al., Predicting biomaterial property-dendritic cell phenotype relationships from the multivariate analysis of responses to polymethacrylates, Biomaterials 33 (6) (2012) 1699–1713.
[126] N. Bhandaru et al., Ordered alternating binary polymer nanodroplet array by sequential spin dewetting, Nano Lett. 14 (12) (2014) 7009–7016.
[127] N. Ferrell, D. Hansford, Fabrication of micro- and nanoscale polymer structures by soft lithography and spin dewetting, Macromol. Rapid. Comm. 28 (8) (2007) 966–971.
[128] S. Herminghaus, K. Jacobs, R. Seemann, Viscoelastic dynamics of polymer thin films and surfaces, Eur. Phys. J. E 12 (1) (2003) 101–110.
[129] D. Beysens et al., Using radiative cooling to condense atmospheric vapor: a study to improve water yield, J. Hydrol. 276 (1–4) (2003) 1–11.